CHAPTER IV

RESULTS AND DISCUSSION

This chapter is divided into two parts: the synthesis and characterization results and the catalytic activity on methanol conversion.

4.1 The synthesis and characterization results

4.1.1 Effect of aging step in synthesis strategy

The synthesis method was based on the Al-SBA-15 synthesis reported by Yue *et al.*[13], that was performed without aging step resulting in the Al-SBA-15 having the XRD pattern with broad peak of hexagonal character and low intensity. However in the original method of pure silica SBA-15 synthesis[11,12], the gel mixture was aged for 20 h at 35 °C and the solid obtained showed well and sharp hexagonal characteristic peak with high intensity.

Figure 4.1 shows the XRD patterns of assynthesized Fe-SBA-15 materials which were prepared with the Si/Fe ratio in gel of 90, the pH in gel about 1.5 and using Fe^{3+} as iron source. No peak was found in the XRD pattern of the material synthesized without aging process, it means that the resulting material is amorphous not crystalline phase. In contrast, the material obtained from preparation with aging step exhibits three characteristic reflection peaks of hexagonal structure of SBA-15 structure and the XRD data with typical assignments of lattice planes are shown in Table 4.1. The results show that the aging is the essential step in the formation of SBA-15 structure. This probably causes from the phenomena occurring during aging process.

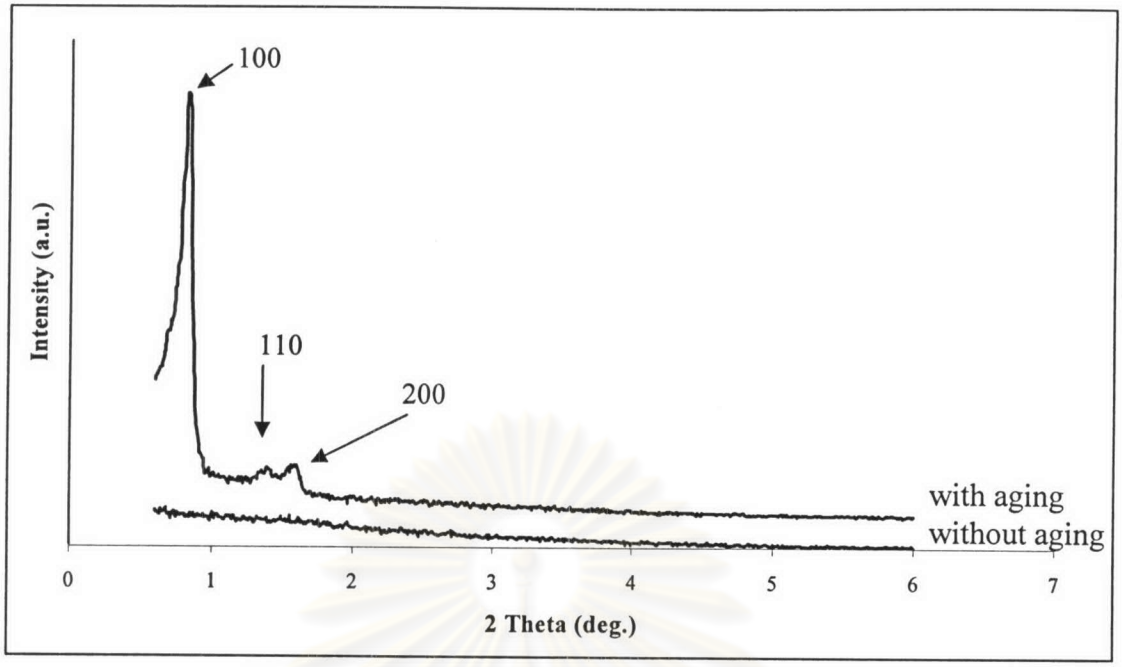

Figure 4.1 XRD patterns of assynthesized Fe-SBA-15 (the Si/Fe ratio in gel of 90) prepared at the pH about 1.5 using Fe^{3+} as iron source with and without aging step.

Table 4.1 The XRD data of the assynthesized Fe-SBA-15

Lattice plane	Bragg's angle, 2θ (degree)	d-spacing (Å)
100	0.82	107.61
110	1.39	63.48
200	1.60	55.15

The hexagonal structure has a characteristic d-spacing ratio given in Equation 2.7 and 2.8. The characteristic d-spacing ratio of perfect hexagonal structure is 1.732 and 2.000 for d_{100}/d_{110} and d_{100}/d_{200}, respectively. For the d-spacing data of synthesized Fe-SBA-15 as shown in Table 4.1, the d-spacing ratio can be calculated:

$$d_{100}/d_{110} = 107.61/63.48 = 1.70$$

and

$$d_{100}/d_{200} = 107.61/55.15 = 1.95.$$

The ratios of synthesized Fe-SBA-15 are slightly different from that of perfect hexagonal structure indicating that the synthesized Fe-SBA-15 is distorted hexagonal structure due to the substitution of iron atoms into the framework of SBA-15.

Many researchers have accepted that during aging period, chemical rearrangements give rise to the formation of nuclei which continuously grow to the crystals, especially aging at room temperature.[94-97] During aging at 40 °C, TEOS used as silica source is slowly hydrolyzed and condensed around the template micelle. On the other hand, without aging step the gel was heated to 100 °C immediately, the hydrolysis rate is high and silica species are independently condensation not around the template that causes the formation of amorphous.

Figure 4.2 and 4.3 show the SEM images of the products synthesized without and with aging step, respectively. Without aging step, the product particles have uncertain feature while those obtained with aging step present more defined feature, donut-like shape. These SEM results are in agreement with the corresponding XRD results in Figure 4.1.

Thus Fe-SBA-15 (Si/Fe = 90 in gel) can be synthesized using the hydrothermal method at the pH about 1.5 with requirement of aging step at 40 °C for 24 h before crystallization. The aging step is added into the synthesis recipe for the rest of study.

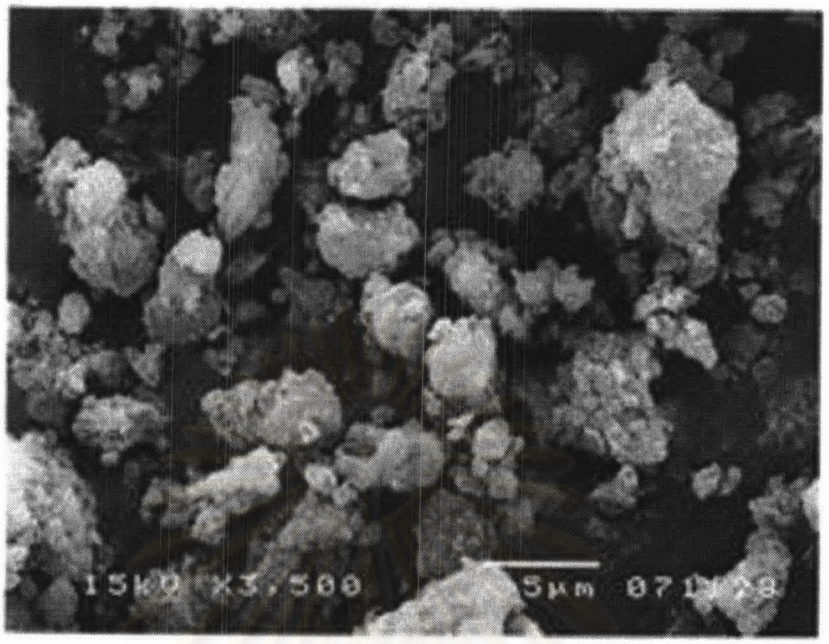

(A)

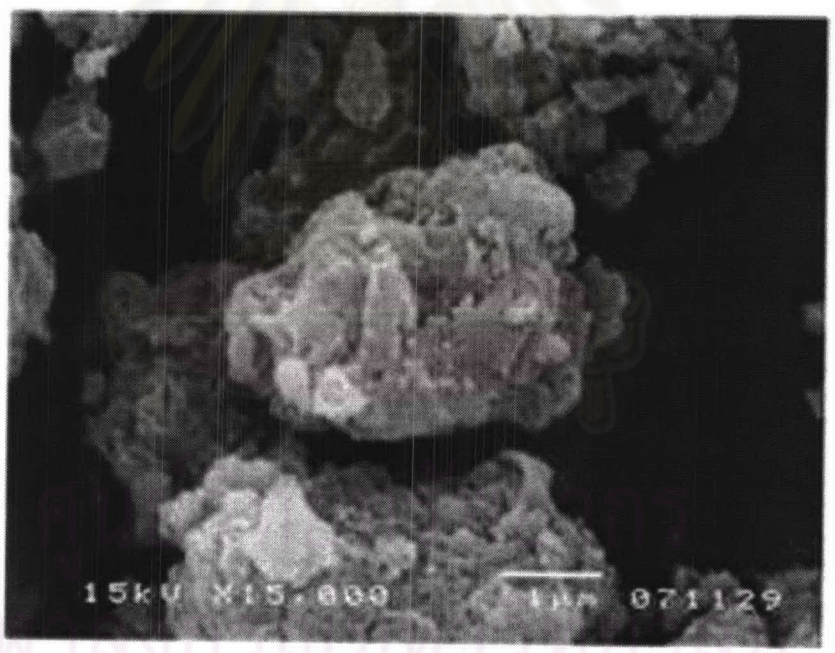

(B)

Figure 4.2 SEM images of as-synthesized Fe-SBA-15 (the Si/Fe ratio in gel of 90) prepared at the pH near 1.5 using Fe^{3+} as iron source without aging step, (A) × 3500 magnification; (B) × 15000 magnification.

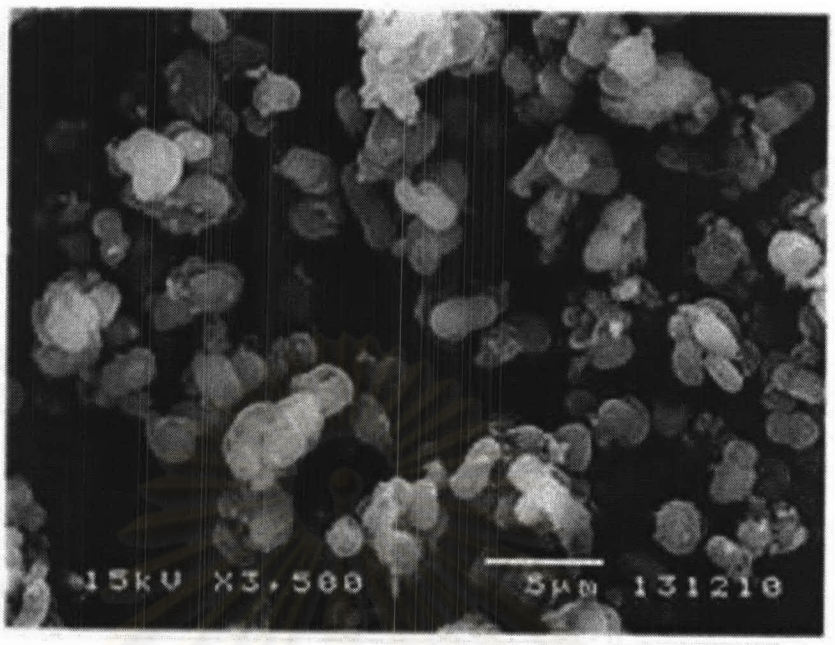

(A)

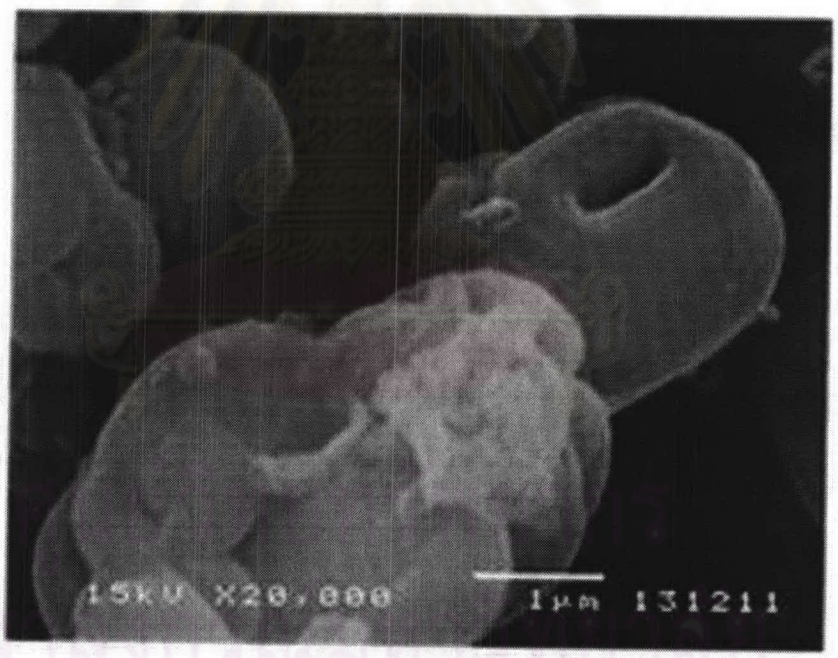

(B)

Figure 4.3 SEM images of as-synthesized Fe-SBA-15 (the Si/Fe ratio in gel of 90) prepared at the pH near 1.5 using Fe^{3+} as iron source with aging step, (A) × 3500 magnification; (B) × 20000 magnification.

4.1.2 The effect of reagent-addition order

This experiment was performed to prove the suggestion that the formation of iron substituted framework materials must be prepared by primary formation of ferrisilicate complexes from a reaction of iron with silica.[31] Thus method I allows the iron source mixed with silica source before added into the template solution, while method II allows that the iron source and the TEOS were separately added into the template directly. In this experiment, both of Fe^{2+} and Fe^{3+} were used as iron source with the Si/Fe molar ratio of 180 and the pH in gel was 2.0.

The XRD patterns and SEM images of the products synthesized by different order of reagent addition are shown in Figure 4.4 and 4.5, respectively. All materials synthesized from method I and method II using Fe^{2+} and Fe^{3+} show no difference in the XRD and SEM image results. XRD patterns of all materials exhibits three characteristic reflection peaks of hexagonal structure and the morphology of all materials is worm-like shape. It shows that the morphology and crystal structure are not affected by different reagent-addition order. The formation of SBA-15 structure should be due to the process during aging step that allows the complete arrangement of silica framework.

To characterize the coordination number of iron in materials, ESR was used for identification. Before measured, the tested material must be calcined to remove templates and moistures in the materials because the template or H_2O molecule can coordinate with the iron atom in material resulting in the wrong coordination data. During calcination process the O_2 must be flowed to transform organic template to CO_2, so any iron species in material are converted to Fe^{3+}. Then the signals in ESR spectra belong to the Fe^{3+} species. The Fe^{2+} and Fe^{3+} labels in Figure 4.6 mean the used iron source, not true iron form.

ESR spectrum of Fe-SBA-15 in Figure 4.6 exhibits two signals: one is at the g value of 2 (right signal) represented the non-framework iron species in the Fe-SBA-15 material and the other one is at the g value of 5 (left signal) assigned to the framework iron.[31] It is obvious that the location of iron in Fe-SBA-15 materials synthesized by two methods are dissimilar although the morphology and crystal structure of Fe-SBA-15 from both methods

are not different. By method I, the ESR spectra show both tetrahedral and octahedral irons found in the materials, it shows that some iron atoms are located in framework position and the rest in non-framework position. By method II, only the signal at g value of 2.0 is found in the spectra, so all iron atoms are located in non-framework position. Premixing of iron and silica source results in which iron atoms are fixed in silicate structure by formation of ferrisilicate complexes. In method II, iron solution and TEOS are not premixed, then iron precipitated separately at the non-framework position while the silicates condense together to form the structure of SBA-15. In this work, the framework iron in SBA-15 structure is desired, so the order in addition of the reagents is performed following method I.

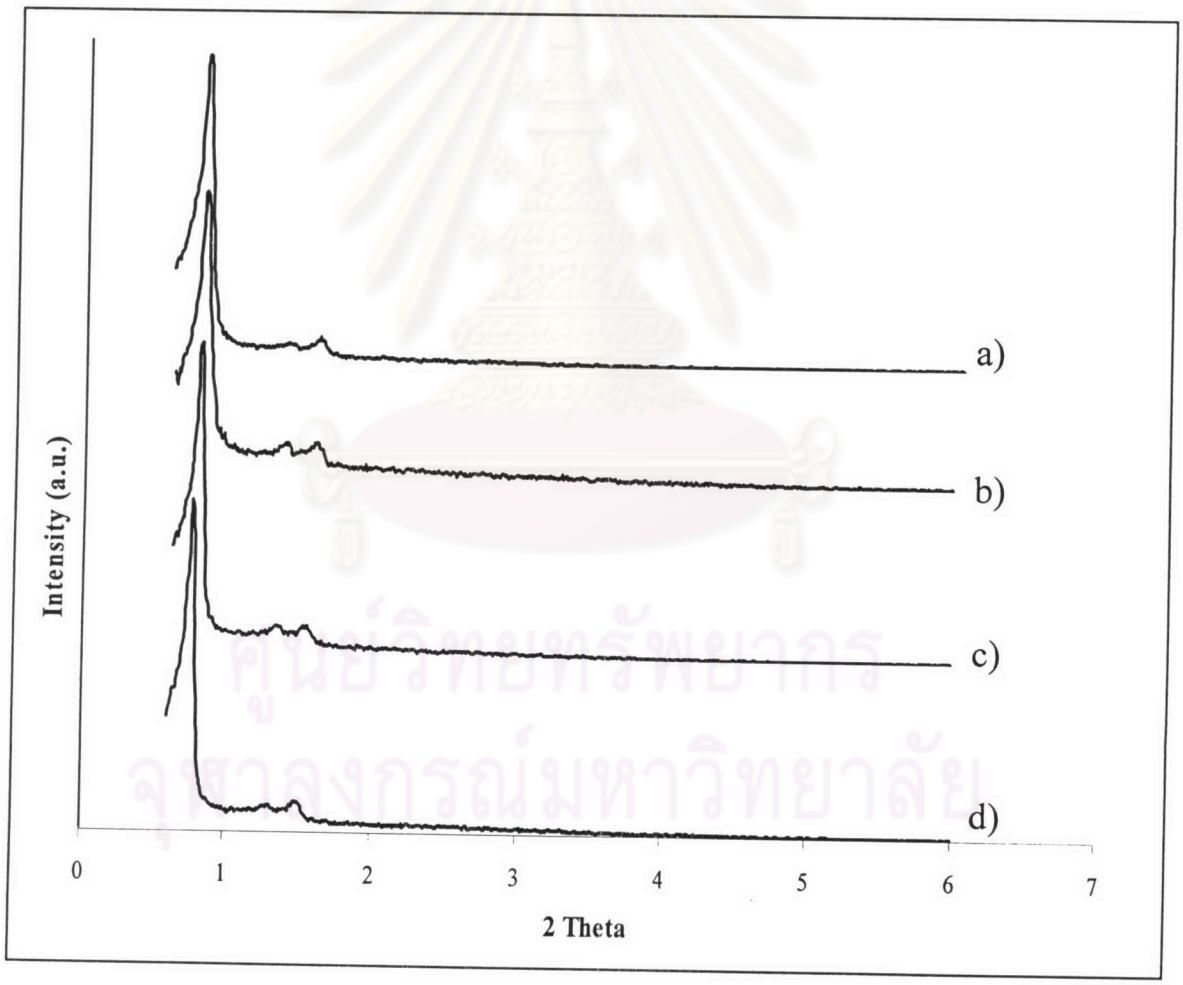

Figure 4.4 XRD patterns of as-synthesized Fe-SBA-15 (the Si/Fe ratio in gel of 180) prepared at the pH of 2.0 in gel using: both a) Fe^{3+} and b) Fe^{2+} by method I, both c) Fe^{3+} and d) Fe^{2+} by method II.

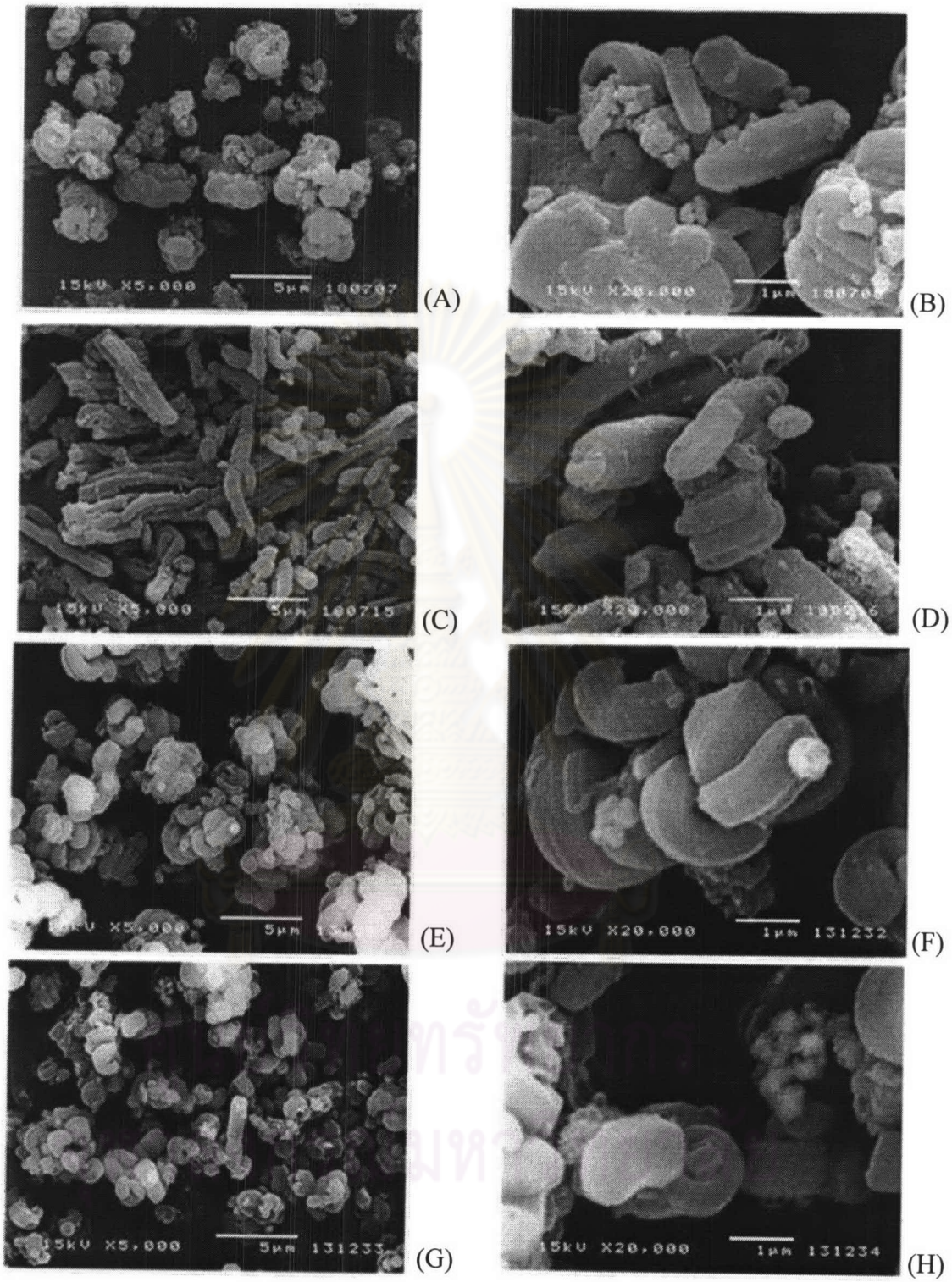

Figure 4.5 SEM images of as-synthesized Fe-SBA-15 (the Si/Fe ratio in gel of 180) prepared at the pH of 2.0 in gel using: (A), (B) Fe^{3+} and (C), (D) Fe^{2+} as iron source synthesized by Method I and (E), (F) Fe^{3+} and (G), (H) Fe^{2+} as iron source synthesized by Method II.

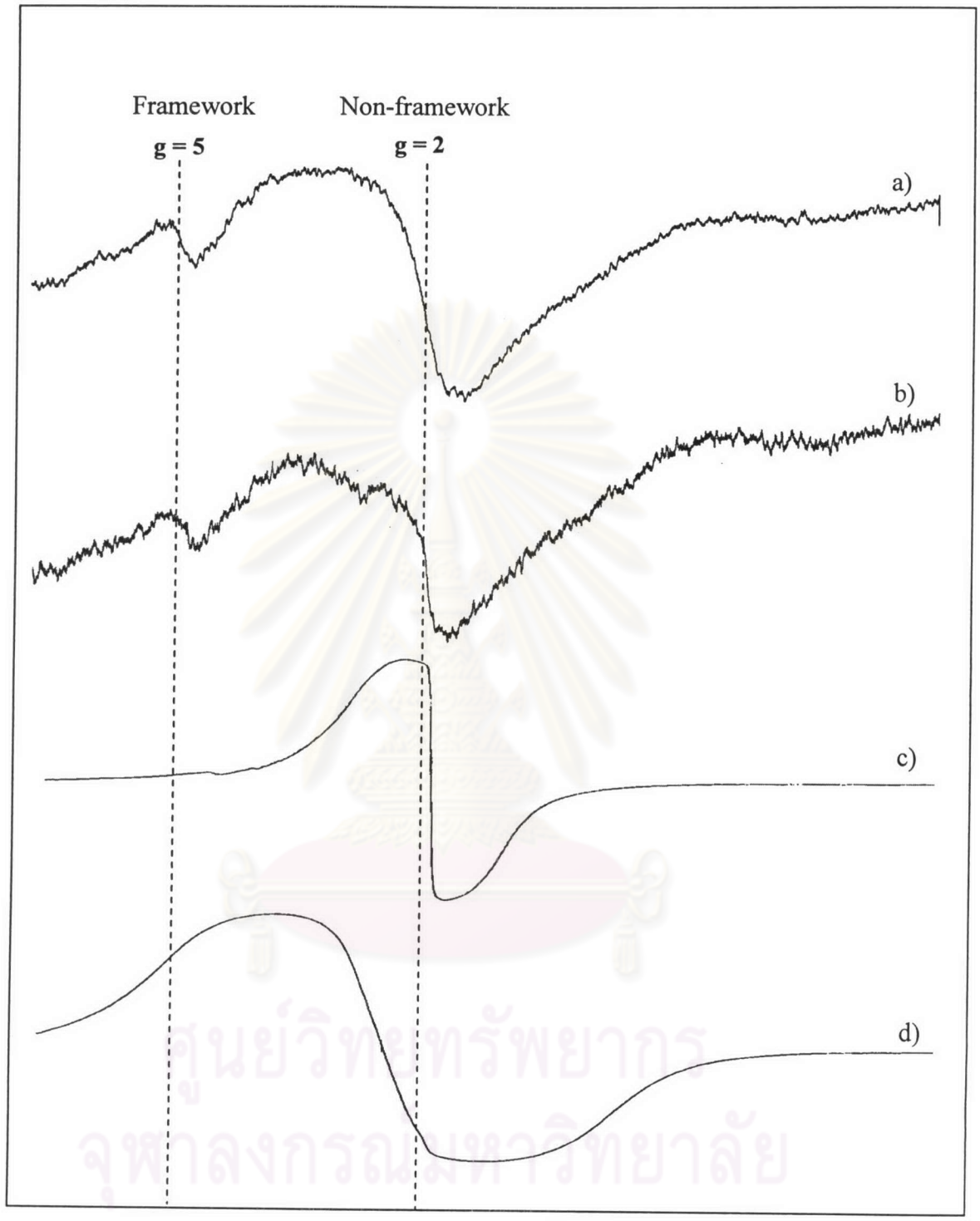

Figure 4.6 ESR spectra of as-synthesized Fe-SBA-15 (the Si/Fe ratio in gel of 180) prepared at the pH of 2.0 in gel using: both a) Fe^{3+} and b) Fe^{2+} by method I, both c) Fe^{3+} and d) Fe^{2+} by method II.

4.1.3 Effects of pH on formation of Fe-SBA-15

From the synthesis of Fe-SBA-15 by method I, the gel pH effect was studied by varying the pH values from 1.0 to 2.5 for every material synthesized by using Fe^{3+} and Fe^{2+} as iron source and the Si/Fe molar ratio of 180 and 90. In addition the pH values of -0.3 and 3.0 were studied in the Fe-SBA-15 material prepared by using Fe^{3+} and the Si/Fe ratio of 180.

4.1.3.1 Effects of pH on Fe-SBA-15 synthesized with Fe^{3+} and the Si/Fe ratio in gel of 180

Figure 4.7 shows the XRD patterns of Fe-SBA-15 synthesized under the following condition: Fe^{3+} as iron source, the Si/Fe ratio in gel 180, and at the pH of -0.3, 1.0, 1.5, 2.0, 2.5, and 3.0. The XRD patterns of materials synthesized at the pH of 1.0 – 2.5 show the sharp intense peaks of 100 and two small peaks of 110 and 200 that are the characteristic pattern of SBA-15 structure. However, the 110 and 200 peaks of Fe-SBA-15 synthesized at the pH of 1.0 are the most resolved among the other samples synthesized at other pH values. It means that the structure of Fe-SBA-15 synthesized at the pH of 1.0 is highly uniform and has the best crystallinity. The XRD pattern of the sample synthesized at the pH of 2.5 looks broader than others. This is in agreement with the literature of the original synthesis method[11,12] of pure silica SBA-15. The crystallinity of SBA-15 was reduced when the pH value was increased due to the weak interaction between template and inorganic species. It can be concluded that the structure of Fe-SBA-15 synthesized at the pH of 1.0 have better crystallinity than that at the pH of 1.5, 2.0, and 2.5, respectively. In addition, the XRD pattern of Fe-SBA-15 synthesized at the pH of 3.0 has one outstanding peak; it proves that the crystallinity of the Fe-SBA-15 is reduced with increasing pH of gel. In addition, the gel pH of -0.30 (approximately 2 M of HCl) was accepted for synthesis of pure silica SBA-15.[11,12] In contrast, the material synthesized at the lowest pH (-0.30) in this work is amorphous because its XRD pattern has no peak.

Moreover, Figure 4.8 shows the SEM images of Fe-SBA-15 synthesized at different pH values with two different magnifications in left and right corresponding to the XRD data in Figure 4.7. At very low pH of -0.30, the material obtained forms amorphous particles like Figure 4.2, even though the mixing gel was aged before crystallization. The result indicates that the formation of the SBA-15 structure also depends on the synthesis condition, in particular pH besides aging process. It is due to the high hydrolysis rate of TEOS in strong acid media and high formation rate of ferrisilicate complexes. The use of strongly acidic solution also stimulates the condensation rate of silica causing the formation of large and disordered complexes. When the ferrisilicate complexes were adding into the template solution, the ordered arrangement of complexes around the template cannot be performed. At higher pH of 1.0-3.0, the morphology of all synthesized products have more defined morphology, i.e. worm-like shape. This shows that at the pH ranged from 1.0 to 3.0 the hydrolysis rate of TEOS and the condensation rate of ferrisilicate complexes are suitable to form the SBA-15 structure.

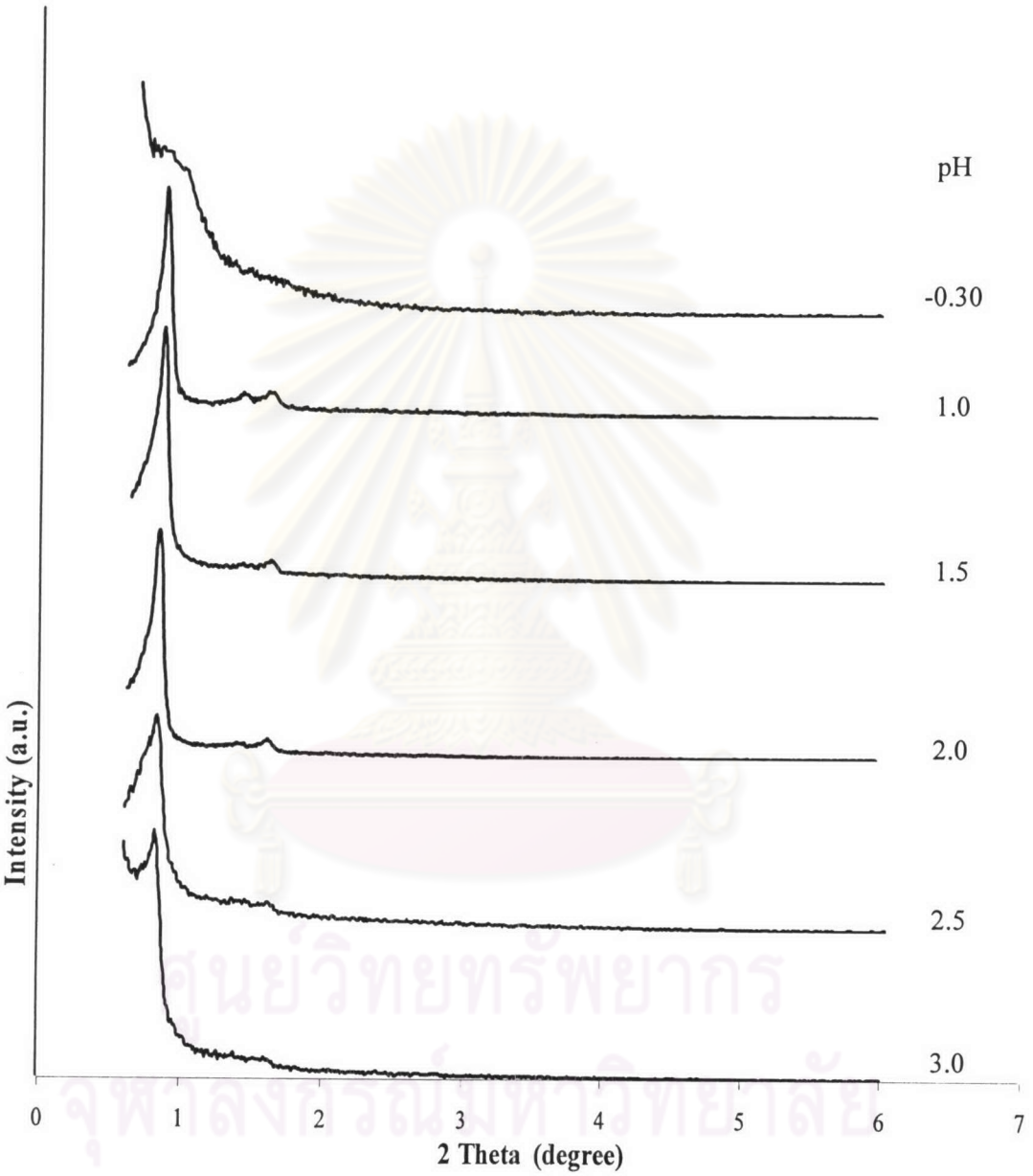

Figure 4.7 XRD patterns of Fe-SBA-15 synthesized with the Si/Fe in gel of 180, Fe^{3+} as iron source, and at various pH values.

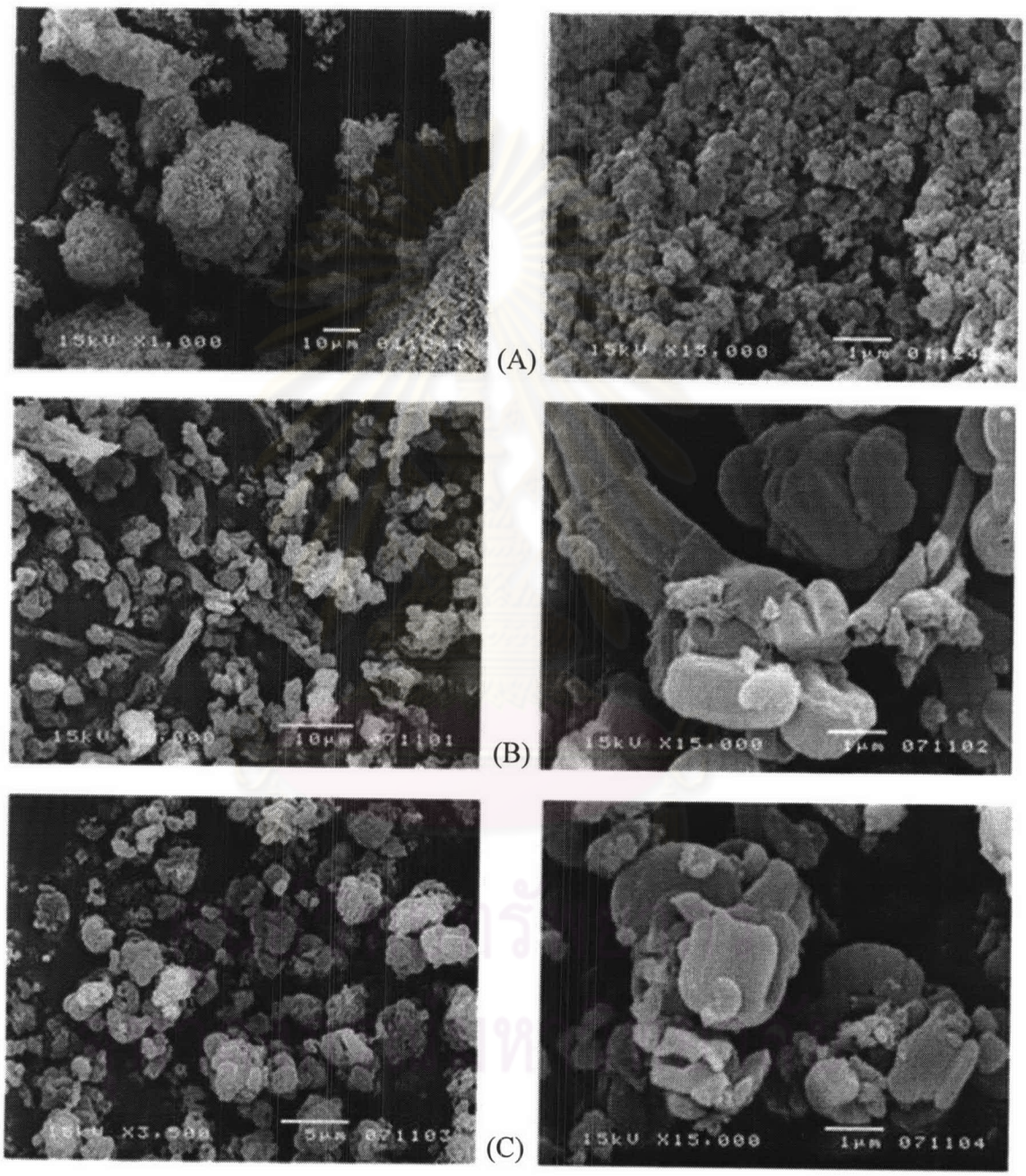

Figure 4.8 SEM images of Fe-SBA-15 synthesized under following conditions: Fe^{3+} as iron source, the Si/Fe in gel of 180, and at various pH values: (A) -0.30, (B) 1.00, (C) 1.50, (D) 2.00, (E) 2.50, and (F) 3.00. Each is shown at two different magnifications (left and right columns).

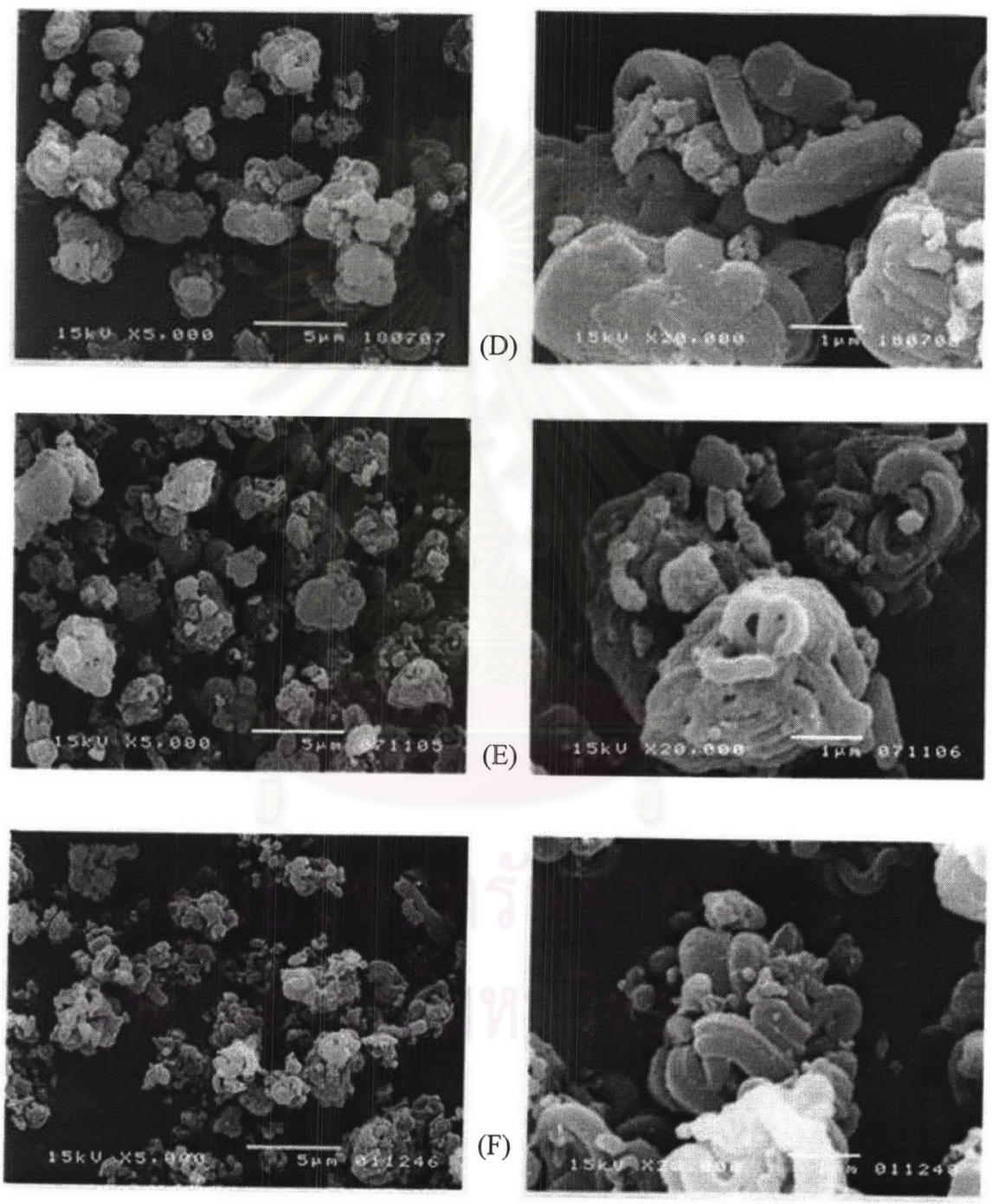

Figure 4.8 (continued).

ESR spectra of the Fe-SBA-15 samples were shown in Figure 4.9. The ESR of amorphous material synthesized at the pH of gel of -0.30 exhibits the non-framework iron at a relative low g value (g = 2.0) and the unidentified iron species at a g value of 7.1. At this pH, Fe-SBA-15 has no iron incorporated in framework observed from no signal at a g value about 5. Moreover, the Fe-SBA-15 synthesized at the pH of 3.00 presents the undefined iron species at a g value of 3.4, as seen in the ESR spectrum in Figure 4.9 (F). In contrast, the ESR spectra of Fe-SBA-15 synthesized at the pH values of 1.0, 1.5, 2.0, and 2.5 show only two signals of framework and non-framework iron species. At the pH of 1.0, the ESR signal shows one signal at g = 2.0, so this Fe-SBA-15 has only non-framework iron. On the other hand, at other pH values both signals at g = 5.0 and 2.0 are found in ESR spectra, thus the Fe-SBA-15 contains both non-framework and framework iron. It can be implied that at lower pH the high solubility of iron hydroxo complexes is accounted for the extremely low iron incorporation.[98] However at higher pH, iron can longer resist to acid and be found in the framework position. From XRD, SEM and ESR results, it can be concluded that the pH values of -0.30 and 3.0 are not proper for preparing Fe-SBA-15, so the test of pH effect of the rest materials are performed at the pH ranged from 1.0 to 2.5.

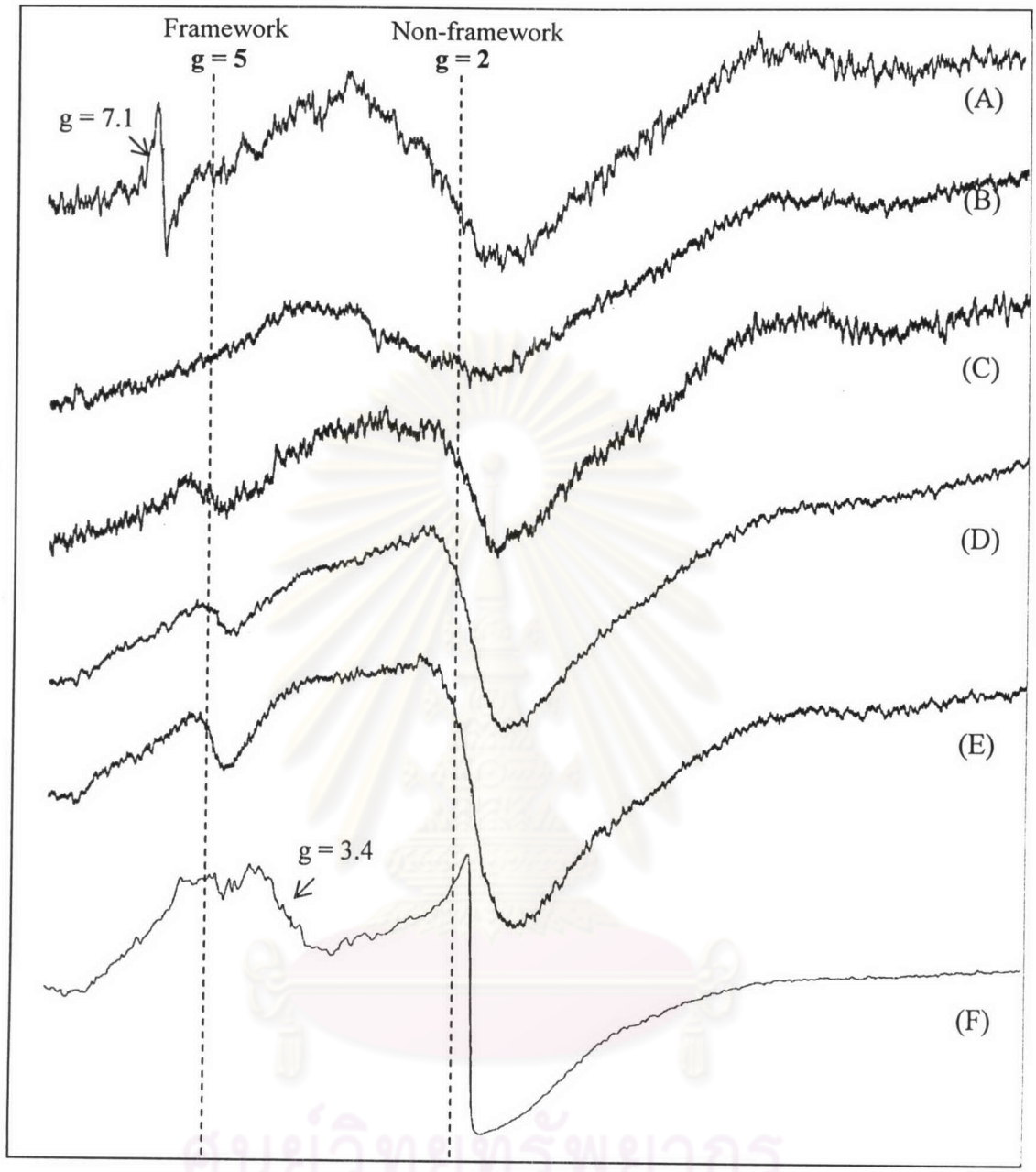

Figure 4.9 ESR images of Fe-SBA-15 which are synthesized under following conditions: Fe^{3+} as iron source, the Si/Fe molar ratio of 180 and at various pH values: (A) -0.30, (B) 1.00, (C) 1.50, (D) 2.00, (E) 2.50, and (F) 3.00.

4.1.3.2 Effects of pH on Fe-SBA-15 synthesized with Fe^{3+} and the Si/Fe ratio in gel of 90

Figure 4.10 and Figure 4.11 show the XRD patterns and the SEM images of Fe-SBA-15 synthesized under the following condition: Fe^{3+} as iron source, the Si/Fe ratio in gel of 90, and at the gel pH values of 1.0, 1.5, 2.0, and 2.5. All materials show the three characteristic peaks of SBA-15 structure that are similar to those of Fe-SBA-15 synthesized with the Si/Fe molar ratio of 180 at various pH values in topic 4.1.3.1. The synthesis at the pH of 1.0 also gives the better crystallinity of Fe-SBA-15 than at the pH values of 1.5, 2.0, and 2.5, respectively. The morphology of all Fe-SBA-15 at various pH values is only worm-like shape, even at the pH of 1.0. Despite no difference in XRD pattern of the materials with the Si/Fe molar ratio of 180 and 90 at the pH of 1.0, there is the contrast in the SEM images that are worm-like and rope-like at the Si/Fe ratio of 180 and only worm-like at the Si/Fe ratio of 90. It shows that sometimes XRD cannot give the complete detail. The difference in the morphology indicates that increasing the amount of iron from the Si/Fe molar ratio of 180 and 90 affects the crystallinity of Fe-SBA-15. It can be concluded that the crystallinity of Fe-SBA-15 is decreased with increasing pH of gel.

The appearance of ESR signals in Figure 4.12 is similar to Figure 4.9. At the pH of 1.0 (Figure 4.12 (A)), iron can readily dissolve in solution rather than form complexes with silicate, although the amounts of iron in solution are increased. For other pH values, the ESR signals also show both framework and non-framework iron characteristics.

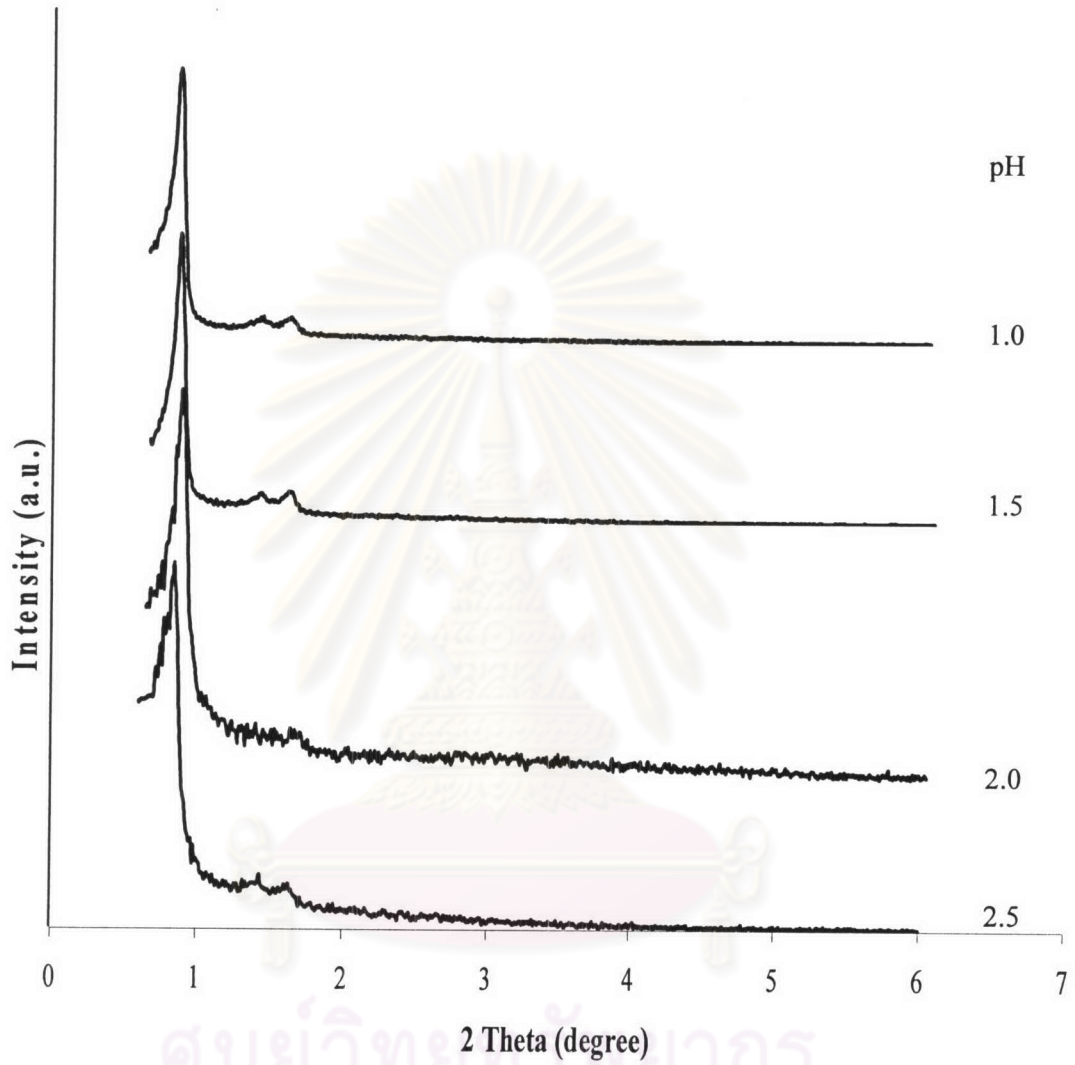

Figure 4.10 XRD patterns of Fe-SBA-15 synthesized at the Si/Fe molar ratio of 90, Fe^{3+} as iron source, and at various pH values of 1.00, 1.50, 2.00, and 2.50.

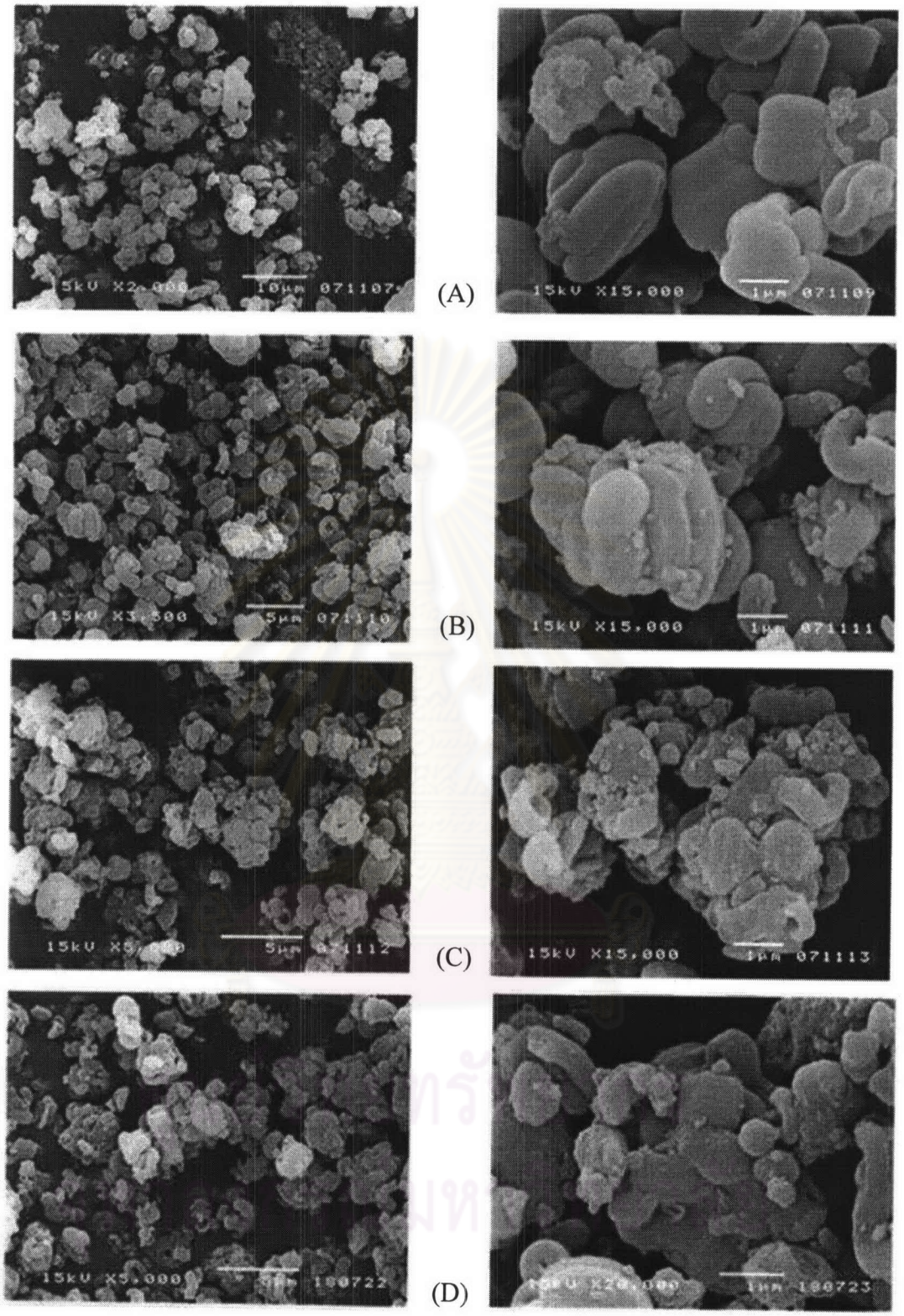

Figure 4.11 SEM images of Fe-SBA-15 synthesized under following conditions: Fe^{3+} as iron source, the Si/Fe in gel of 90, and at various pH values: (A) 1.00, (B) 1.50, (C) 2.00, and (D) 2.50. Each is shown at two different magnifications (left and right columns).

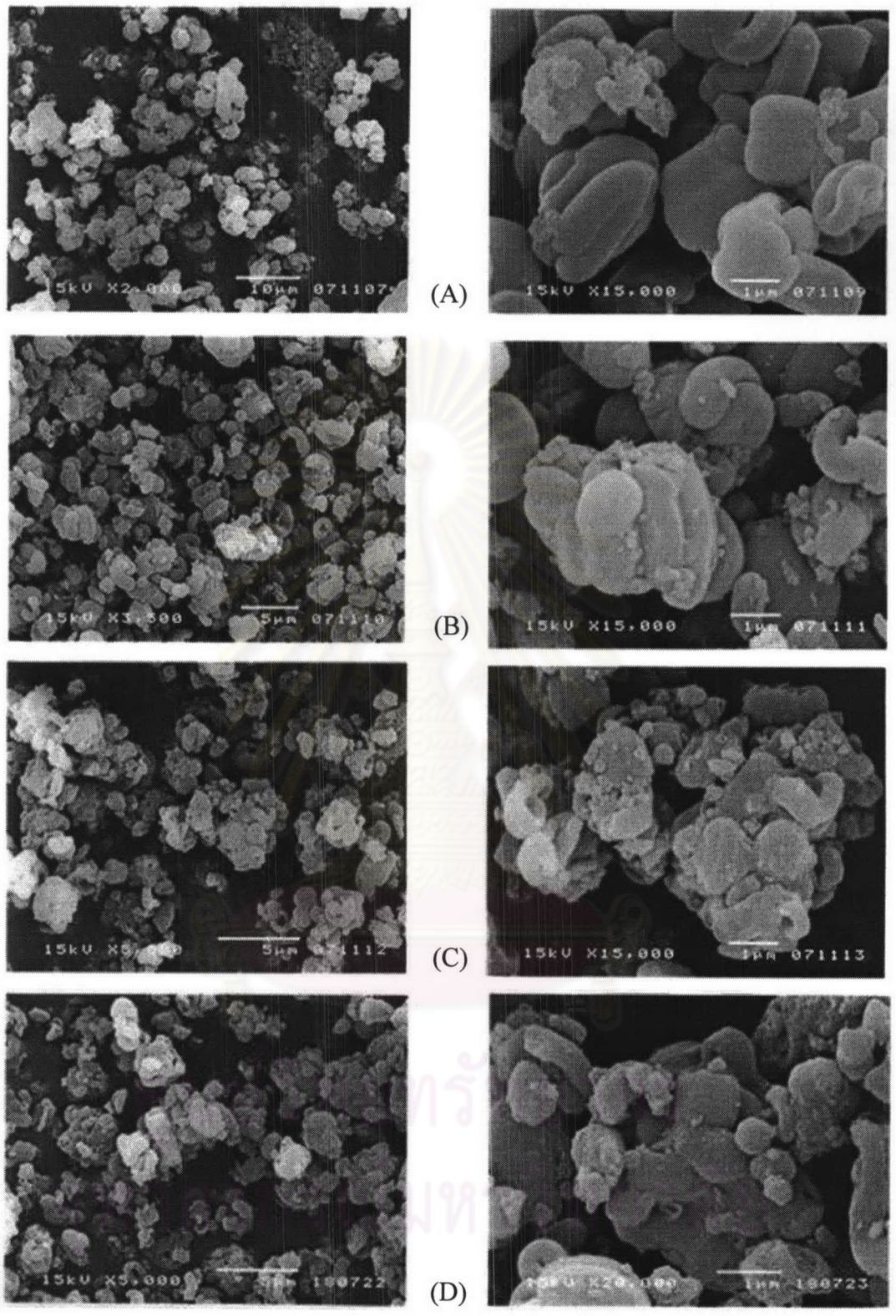

Figure 4.11 SEM images of Fe-SBA-15 synthesized under following conditions: Fe^{3+} as iron source, the Si/Fe in gel of 90, and at various pH values: (A) 1.00, (B) 1.50, (C) 2.00, and (D) 2.50. Each is shown at two different magnifications (left and right columns).

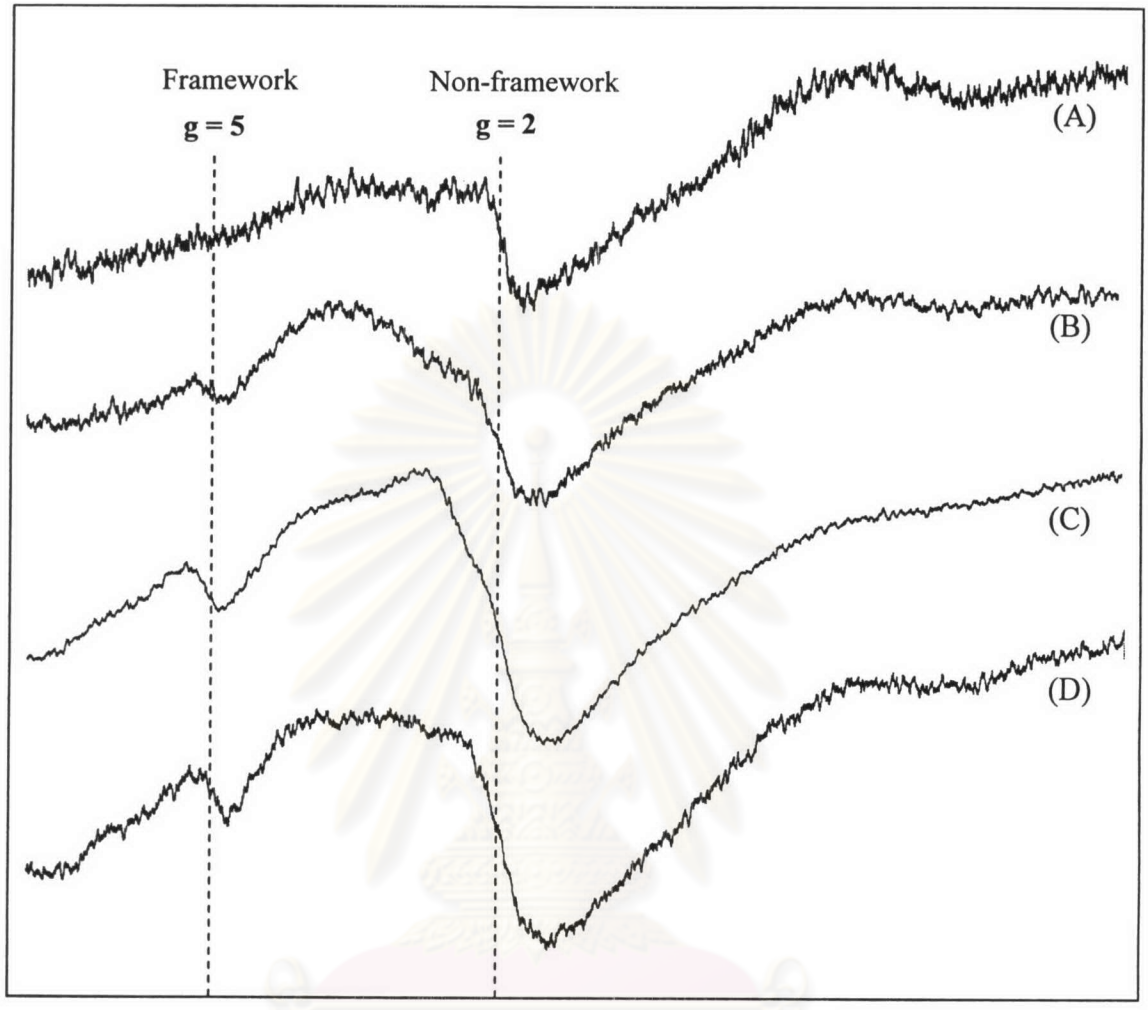

Figure 4.12 ESR images of Fe-SBA-15 which are synthesized under following conditions: Fe^{3+} as iron source, the Si/Fe molar ratio of 90 and at various pH values: (A) 1.0, (B) 1.5, (C) 2.0, and (D) 2.5.

4.1.3.3 Effects of pH on Fe-SBA-15 synthesized with Fe^{2+} and the Si/Fe ratio in gel of 180

For this experiment, Fe^{2+} was used as iron source instead of Fe^{3+}. Figure 4.13 and Figure 4.14 show XRD patterns and SEM images of Fe-SBA-15 synthesized under the following condition: Fe^{2+} as iron source, the Si/Fe in gel 180, and at the gel pH of 1.0, 1.5, 2.0, and 2.5. All materials show the three well defined hexagonal characteristic peaks in XRD patterns corresponding to the well defined morphology in Figure 4.14. The rope-like shape which is found in all samples suggests that the crystallinity of Fe-SBA-15 synthesized with the Si/Fe molar ratio of 180, with Fe^{2+} as iron source is high.

From ESR spectra in Figure 4.15, all materials exhibit the same signals as those found in Figure 4.9, except the material synthesized at the pH of 1.5 shows only non-framework signal. However, the signals for the pH of 2.0 and 2.5 in Figure 4.15 are not different from that from those in Figure 4.9. It indicates that iron(II) is more difficult to incorporate into the framework than iron(III) at low pH, but at high pH the incorporation capability of iron (II) is close to that of iron (III).

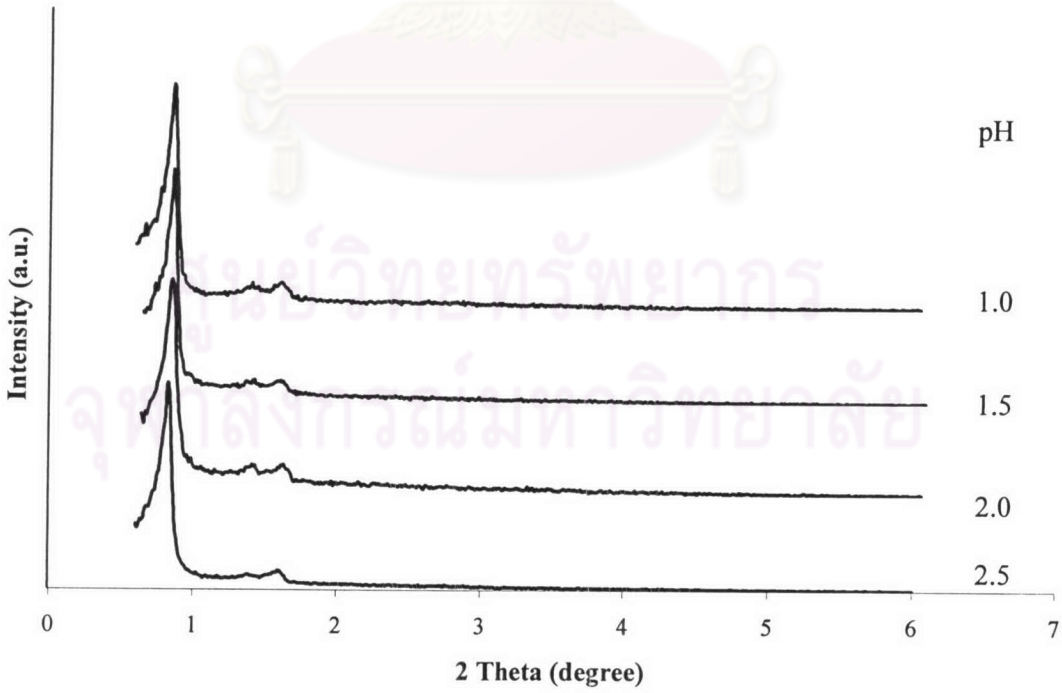

Figure 4.13 XRD patterns of Fe-SBA-15 synthesized with the Si/Fe molar ratio of 180, Fe^{2+} as silica source, at various pH values of 1.0, 1.5, 2.0, and 2.5.

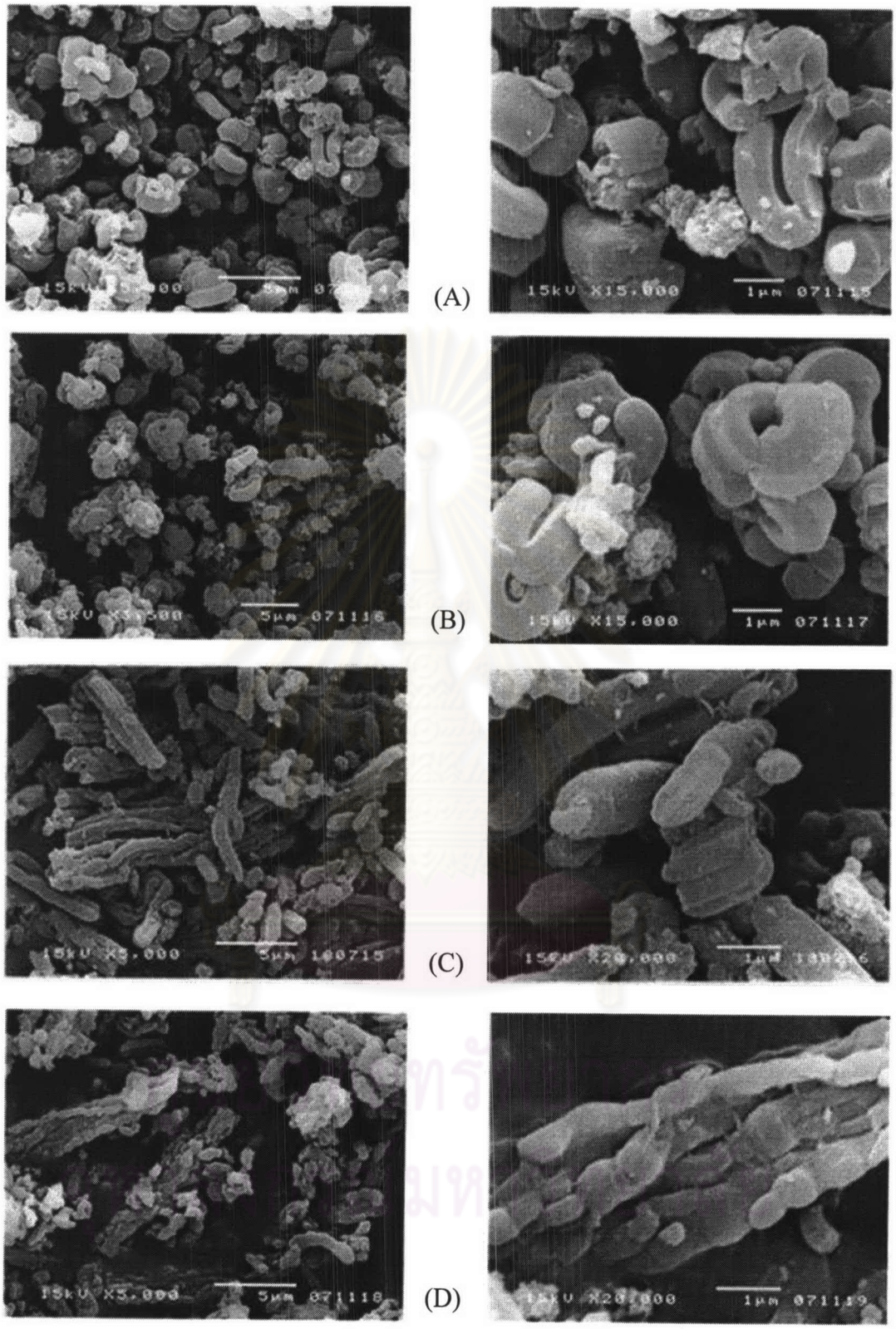

Figure 4.14 SEM images of Fe-SBA-15 synthesized under following conditions: Fe^{2+} as iron source, the Si/Fe in gel of 180, and at various pH values: (A) 1.0, (B) 1.5, (C) 2.0, and (D) 2.5. Each is shown at two different magnifications (left and right columns).

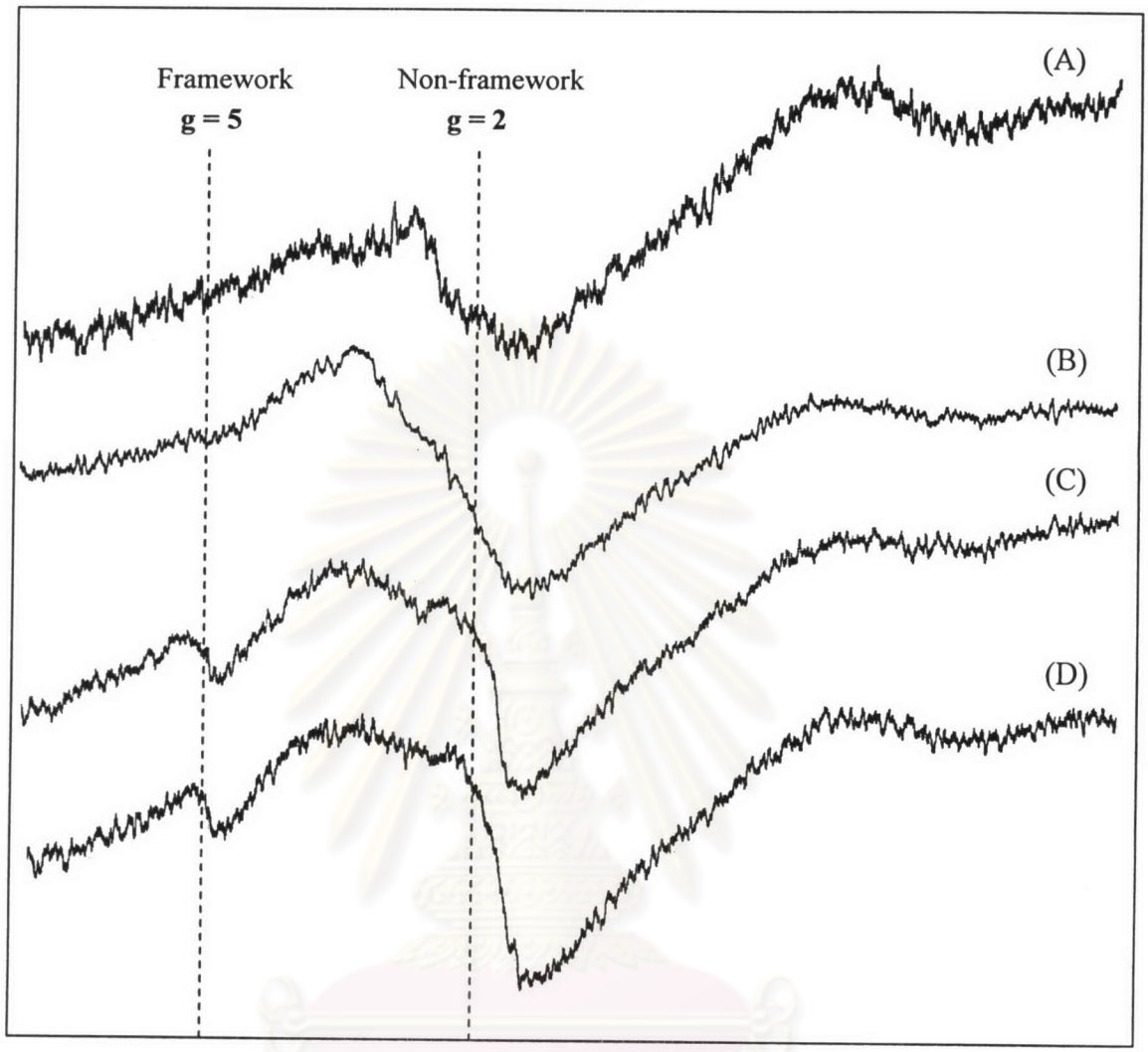

Figure 4.15 ESR images of Fe-SBA-15 which are synthesized under following conditions: Fe^{2+} as iron source, the Si/Fe molar ratio of 180 and at various pH values: (A) 1.0, (B) 1.5, (C) 2.0, and (D) 2.5.

4.1.3.4 Effects of pH on Fe-SBA-15 synthesized with Fe^{2+} and the Si/Fe ratio in gel of 90

XRD patterns of Fe-SBA-15 sample, synthesized using Fe^{2+} as iron source, with the Si/Fe ratio in gel of 90, and at various pH values in range of 1.0-2.5, are shown in Figure 4.16 and SEM results are in Figure 4.17. The three hexagonal characteristic XRD peaks are found for all samples as well as the morphology of all materials is worm-like shape, except at the pH of 1.0 that both rope-like and worm-like morphologies are found. The results indicate that the Fe-SBA-15 material can be synthesized at the pH in range of 1.0 - 2.5.

ESR signals of Fe-SBA-15 synthesized at various pH values are shown in Figure 4.18. Fe-SBA-15 synthesized at the pH values of 1.0 and 1.5 also has only non-framework iron. At the pH of 2.0 and 2.5, iron was found in both framework and non-framework coordination sites. The results above only determine the structural information of the SBA-15 framework. They do not indicate whether and how many ion atoms are incorporated in the SBA-15 structure. The Si/Fe ratios in Fe-SBA-15 synthesized are decreased with increasing pH of the synthesis gel. The amount of incorporated iron will be discussed in the next section.

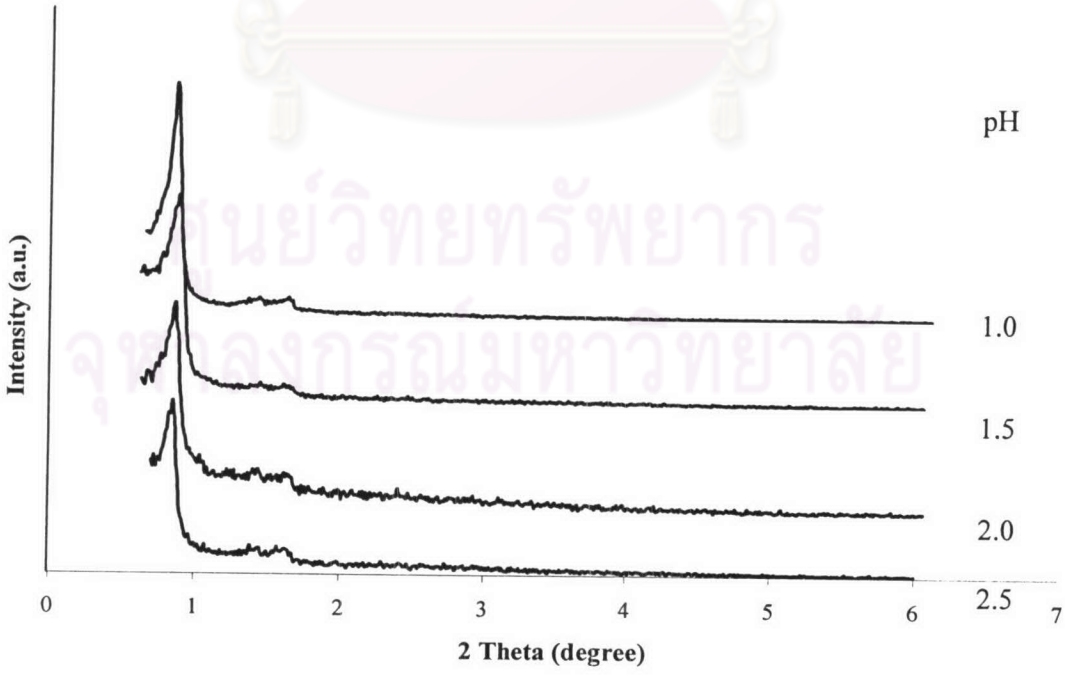

Figure 4.16 XRD patterns of Fe-SBA-15 synthesized at the Si/Fe molar ratio of 90, Fe^{2+} as silica source, and at various pH values of 1.0, 1.5, 2.0, and 2.5.

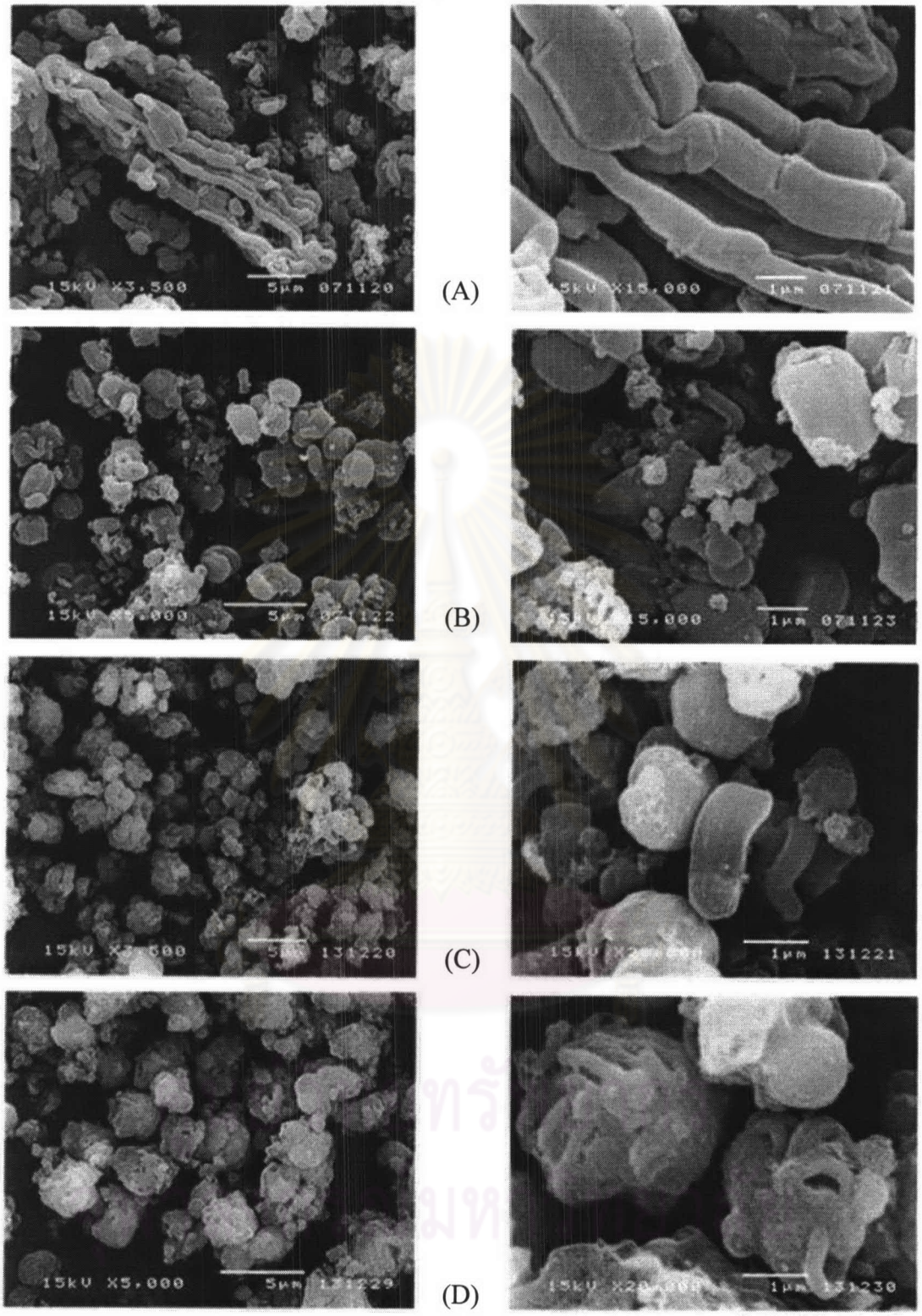

Figure 4.17 SEM images of Fe-SBA-15 synthesized under following conditions: Fe^{2+} as iron source, the Si/Fe in gel of 90, and at various pH values: (A) 1.0, (B) 1.5, (C) 2.0, and (D) 2.5. Each is shown at two different magnifications (left and right columns).

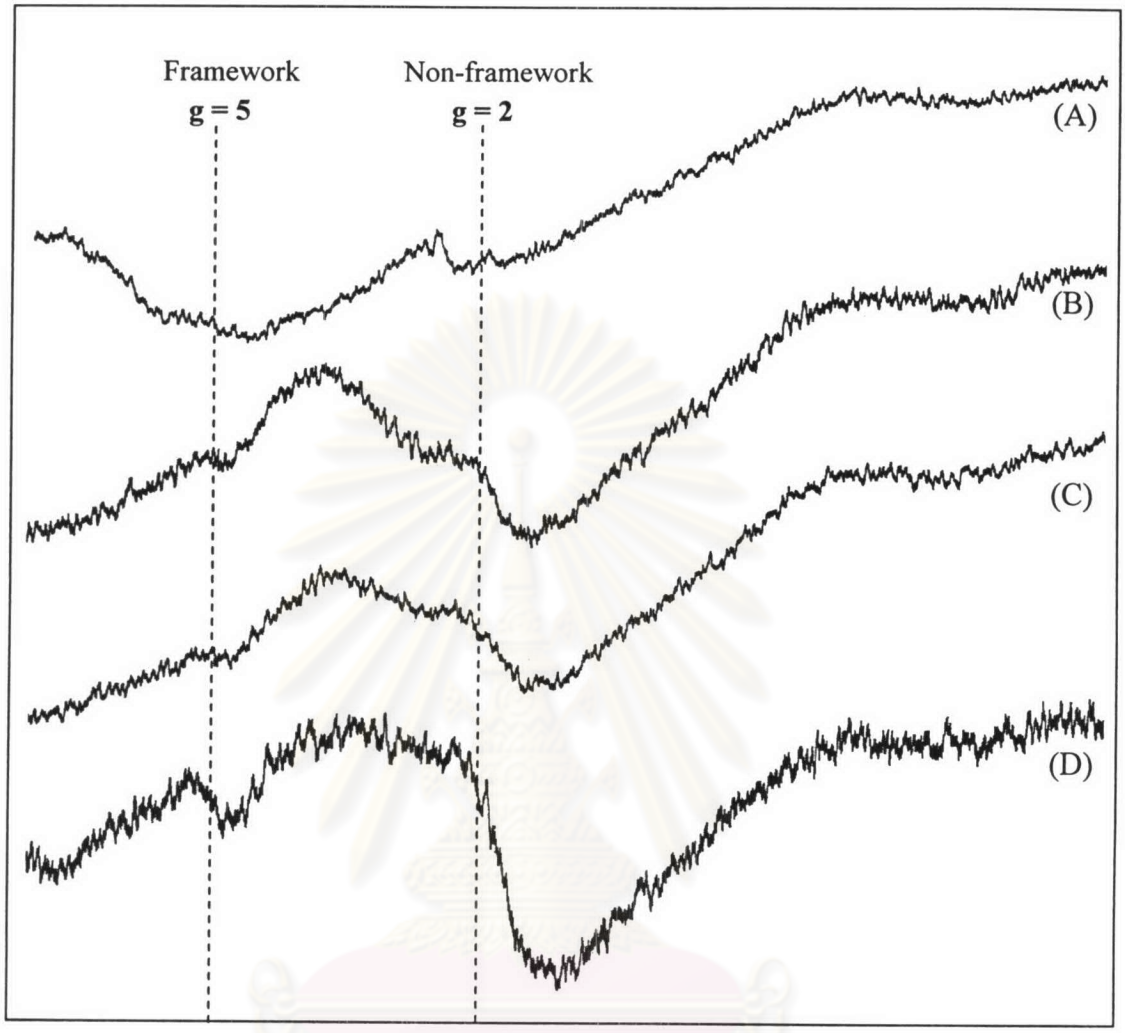

Figure 4.18 ESR images of Fe-SBA-15 synthesized under following conditions: Fe^{2+} as iron source, the Si/Fe molar ratio of 90 and with various pH values: (A) 1.0, (B) 1.5, (C) 2.0, and (D) 2.5.

4.1.3.5 Effect of pH on the iron incorporation

Not only the crystallinity of materials but also the amount of iron incorporated in the materials synthesized is affected by the pH of the synthesis gel. The relative intensities of the ESR signals (g = 5 and 2) assigned to framework and non-framework iron sites, respectively, imply the relative amount of such iron sites. If summations of both ESR signal intensities are normalized to 100, each signal is then related to the percentage amount of the site. The values of Si/Fe ratios and the implicated relative amounts of framework and non-framework iron sites found in Fe-SBA-15 synthesized are concluded in Table 4.2. It is obvious that non-framework site is more predominant than framework site. With increasing the pH of gel, iron can be incorporated in a greater total amount, resulting in lower Si/Fe ratio in material. However, iron site distribution is slightly different among the pH values varied from 1.5 to 2.5.

Table 4.2 Elemental analysis results of Fe-SBA-15 and assignments of iron sites obtained from ESR data.

Fe source	Si/Fe in gel	pH of gel	Si/Fe in material	ESR signal	
				% Framework	% Non-framework
Fe^{3+}	180	1.0	8434	0.0	100.0
		1.5	2280	18.6	81.4
		2.0	345	16.8	83.2
		2.5	223	16.6	83.4
	90	1.0	5371	0.0	100.0
		1.5	1191	18.2	81.8
		2.0	229	15.3	84.7
		2.5	118	20.6	79.4
Fe^{2+}	180	1.0	7711	0.0	100.0
		1.5	1058	0.0	100.0
		2.0	497	21.9	78.1
		2.5	222	16.5	83.5
	90	1.0	6481	0.0	100.0
		1.5	886	21.1	78.9
		2.0	387	10.3	89.7
		2.5	293	22.2	77.8

Note:

$$\% \text{ Framework} = \frac{I_{framework}}{I_{framework} + I_{non\text{-}framework}} \times 100$$

$$\% \text{ Non-framework} = \frac{I_{non\text{-}framework}}{I_{framework} + I_{non\text{-}framework}} \times 100$$

where $I_{framework}$ is intensity of tetrahedral signal at g value of 5 from ESR and $I_{non\text{-}framework}$ is intensity of octahedral signal at g value of 2 from ESR.

4.1.4 Effects of iron source on the formation of Fe-SBA-15

From the XRD patterns in Figure 4.7 and Figure 4.10 comparing with Figure 4.13 and Figure 4.16, all Fe-SBA-15 synthesized from both Fe^{2+} and Fe^{3+} show well-defined hexagonal characteristic peaks of SBA-15 structure. There is no significant difference in the XRD patterns. However, the morphology of Fe-SBA-15 synthesized from Fe^{2+} shows greater amount of rope-like shape than that from Fe^{3+}. It indicates that Fe^{2+} disrupts the Fe-SBA-15 structure less than Fe^{3+} does. This is probably due to less amount of iron incorporated into the framework observed from ESR signal in Figure 4.15 (B) and 4.18 (B) of Fe-SBA-15 synthesized from Fe^{2+} and at the pH of 1.5.

4.1.5 Effects of iron source on the iron content in materials

At the same pH and Si/Fe molar ratio, the data from Table 4.2 reveal that the difference of iron source slightly affects the iron content in material, especially at high pH. This is accounted by that some Fe^{2+} ions are oxidized to Fe^{3+} during crystallization in Teflon that observes from the change of solution color (light green to yellow). Thus the iron contents obtained from two iron sources are not significantly different.

4.1.6 Effects of Si/Fe in gel on the formation of Fe-SBA-15 and iron content in material

Table 4.2 shows that an increase of iron loading with Si/Fe molar ratio in gel from 180 to 90 can increase the content of iron in materials. However, when the Si/Fe molar ratio is decreased to 30 at the pH of 2.5 and using Fe^{3+} as iron source, the morphology of the obtained material is nearly amorphous as shown in Figure 4.19 (A). There are a few worm-like shapes observed in the SEM image. Moreover, pure silica SBA-15 was also synthesized at the same condition and with the Si/Fe molar ratio of ∞ (no iron in gel). Its SEM images are illustrated in Figure 4.19 (D). Comparing with the morphologies in Figure 4.19, the SEM images (C) and (D) are quite similar and present the highest crystallinity (B)

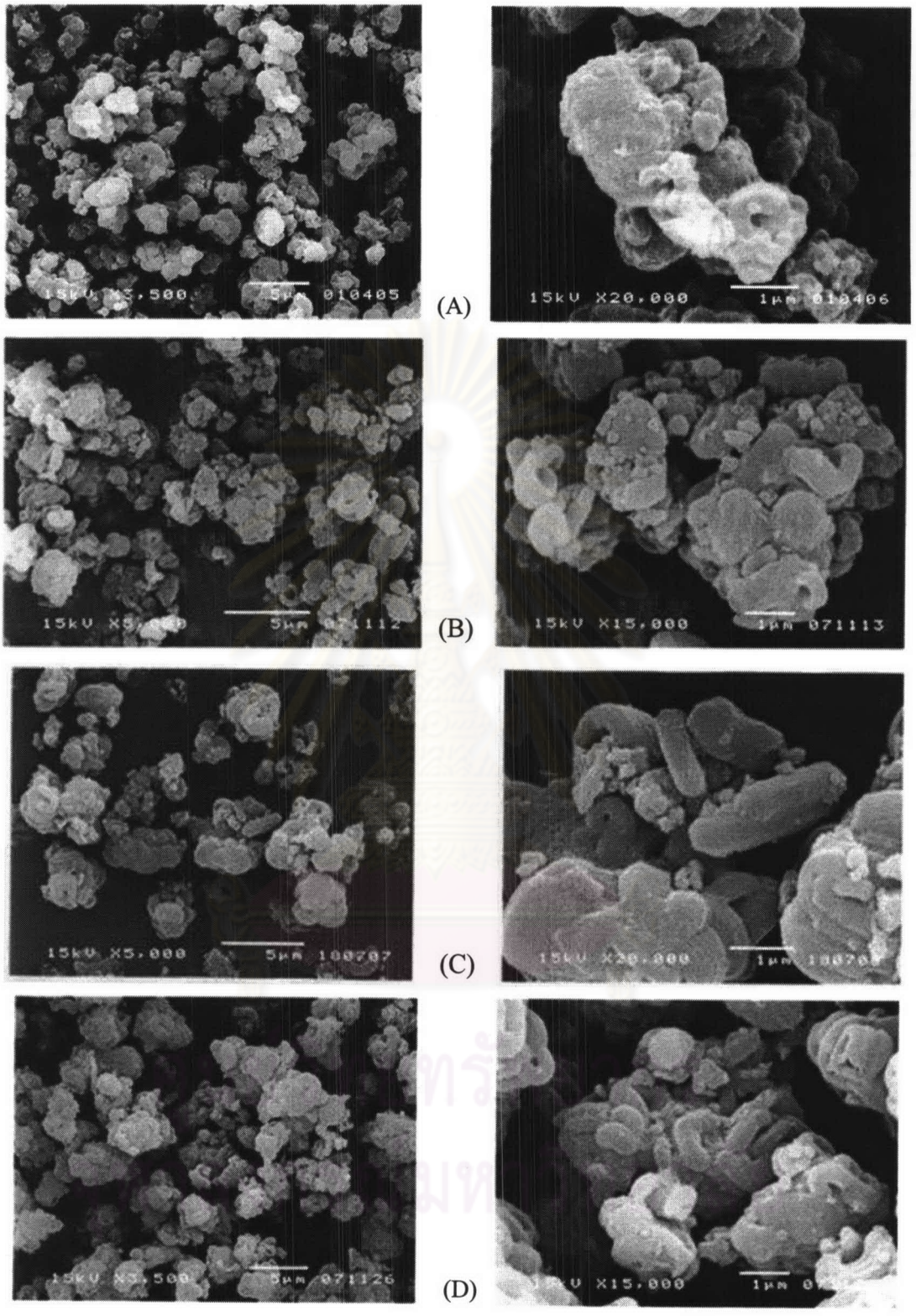

Figure 4.19 SEM images of Fe-SBA-15 synthesized at the pH of 2.5, with Fe^{3+} as iron source, and at the Si/Fe molar ratios of (A) 30, (B) 90, (C) 180, and (D) ∞ or pure silica.

and the lowest crystallinity in (A). This supports the suggestion that the increase of iron quantity in gel provides the lower crystallinity of material.

4.2 Activity test of Fe-SBA-15 for the methanol conversion

According to previous work of our research group, the values of GHSV and TOS for methanol-to-hydrocarbons catalysis has been investigated.[99,100] The activity is optimized at a GHSV of 2000 h^{-1} and TOS of 30 min. The same conditions were used throughout this work on the purpose of comparison in the future.

4.2.1 Effects of temperature on the methanol conversion

To investigate the effects of temperature on the methanol conversion, the blank test and catalytic test were performed at the temperatures of 300, 400, and 500 °C.

4.2.1.1 Blank test

The blank test was operated under the same condition as for the catalytic test, but no catalyst was placed in the tubular reactor. The data for the blank test are shown in Table 4.3 and gas product distribution is shown in Figure 4.20. The percentage conversion shows the quantity of methanol converted to other products. For the blank test, it was found that methanol conversion can occur by pyrolysis even without catalyst. The conversion is the highest at 500 °C, while the lowest conversion is obtained at 300 °C. Then it can be concluded that the conversion of methanol increases with raising the reaction temperature. The unreacted methanol is trapped within the liquid trap immersed under a dry ice-acetone bath.

The products are collected as liquid products in the cold trap and gas products in the Tedlar bag. Percentage selectivity to gas products is raised with increasing temperature, while percentage selectivity to liquid products is reduced. It is reasonable that the first step of the mechanism for methanol conversion is the generation of dimethylether (CH_3OCH_3) (b.p. = 24 °C) which occurs even at low temperature without catalyst. The

transformation of methanol to gas products increases with the reaction temperature yielding higher selectivity to gas products and lower selectivity to liquid products. However, at all temperatures, the selectivity to liquid products is higher than that to gas products. For the analysis of liquid collected in the cold trap, it was found that the most liquid in trap is unreacted methanol and trace amount of liquid products obtained at all reaction temperatures. It is due to two possible reasons. Firstly, because the conversion of methanol is low (less than 21%), the amounts of liquid products are small. For the other reason, one of the liquid products is H_2O which is generated during the formation of dimethylether, so it cannot be detected by flame ionization detector (FID) of GC. For these reasons, the quantities of liquid products are hardly detected. For gas product distribution obtained from the blank test in Figure 4.20, at the temperatures of 400 and 500 °C, methane is the major component (> 80 %) while at 300 °C several types of products are found. It indicates that at high temperature formation of methane is favorable.

Table 4.3 Percentage conversion and product distribution obtained from the blank test of methanol conversion at various temperatures (Conditions: no catalyst, GHSV = 2000 h^{-1}, T_{MeOH} = 35°C, and TOS = 30 min)

	Reaction temperature (°C)		
	300	400	500
%Conversion of methanol	11.58	14.52	20.27
% Product distribution, selectivity to:			
- Gas product (%wt.)	28.27	37.99	49.71
- Liquid product (%wt.)	71.73	62.01	51.29

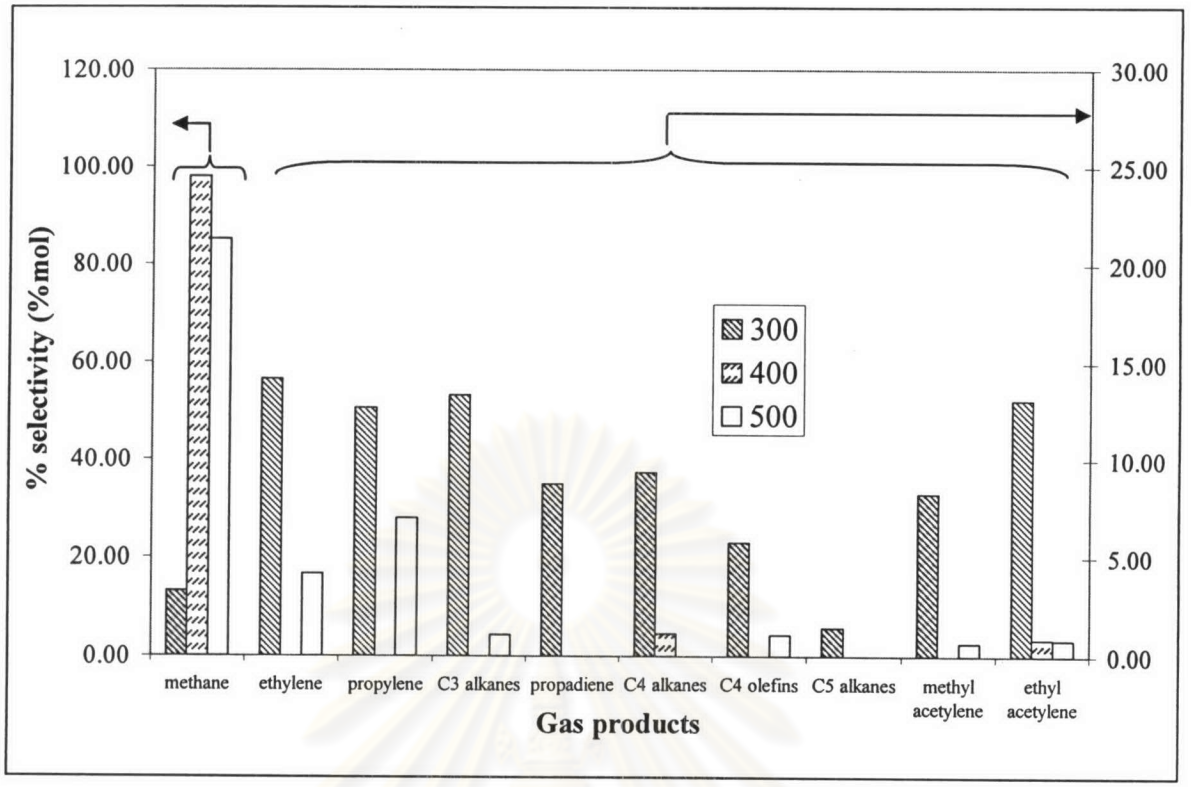

Figure 4.20 The gas product distribution obtained from the blank test of the methanol conversion at various temperatures and other conditions are the same as shown in Table 4.3.

4.2.1.2 Catalytic test over Fe-SBA-15

The Fe-SBA-15 sample synthesized under the following conditions: pH in gel of 2.5, Si/Fe molar ratio in gel of 90, and Fe^{3+} as iron source is used as catalyst for methanol conversion because it has the highest amount of iron in material (Si/Fe = 118). It should be noted that the iron atoms are related to the Brønsted acid sites on the catalyst. The highest iron content in catalyst should give the highest activity in methanol conversion catalyzed by an acid catalyst. The catalytic results over the catalyst at various temperatures are shown in Table 4.4 and Figure 4.21.

From Table 4.4, the percentages conversions of reactions at all temperatures are higher than those obtained from the blank test, even at 300 °C. This proves that Fe-SBA-15 is an active catalyst for methanol conversion. The conversion depends on the

reaction temperature. At 500 °C, 80 % of methanol feeds are converted to products, whereas at 400 and 300 °C the conversions are reduced to 60 and 27%, respectively.

Three phases of products are formed as liquids in cold trap, gases in the Tedlar bag, and coke deposited on the catalyst. The highest amount of coke is found at 300 °C where methanol is just decomposed to coke and methane and some is transformed to other hydrocarbons. With increasing temperature to 400 °C, the catalyst is more active and able to convert methanol to other products, resulting the reduction of coke. However, the amount of coke at 500 °C is higher than at 400 °C because at the reaction temperature of 500 °C the coke can be generated from other side reactions such as cracking of hydrocarbon. For the liquid products, the GC analysis shows that the liquids in the cold trap are the unreacted methanol mainly, while the liquid products are hardly found.

For the gas product distribution which is shown in Figure 4.21, methane is the major component in gas products at all reaction temperatures. Methane is less valuable, while olefins are needed in petrochemical industries. At the temperature of 300 °C, the percentage yield of methane is minimized and those of ethylene, propylene, and butane are maximized. Although the conversion of methanol at 300 °C is only 27 %, the unreacted methanol in the cold trap can be recovered to use as reactant whereas at higher temperature the methanol is converted to worthless methane. Therefore, the next experiment was operated at the reaction temperature of 300 °C.

Table 4.4 Percentage conversion, product distribution, and coke content obtained from the methanol conversion over Fe-SBA-15 (Si/Fe in catalyst = 118 and Fe^{3+} as iron source) at various temperatures (Conditions: 0.25 g of catalyst, GHSV = 2000 h^{-1}, T_{MeOH} = 35°C, and TOS = 30 min)

	Reaction temperature (°C)		
	300	400	500
%Conversion of methanol	27.07	60.68	80.41
% Product distribution selective to:			
- Gas product yield (%wt.)	57.96	71.85	79.21
- Liquid product yield (%wt.)	7.80	18.55	3.36
- Coke yield (%wt)	34.24	9.60	17.43
% Coke based on catalyst	4.28	2.70	7.58

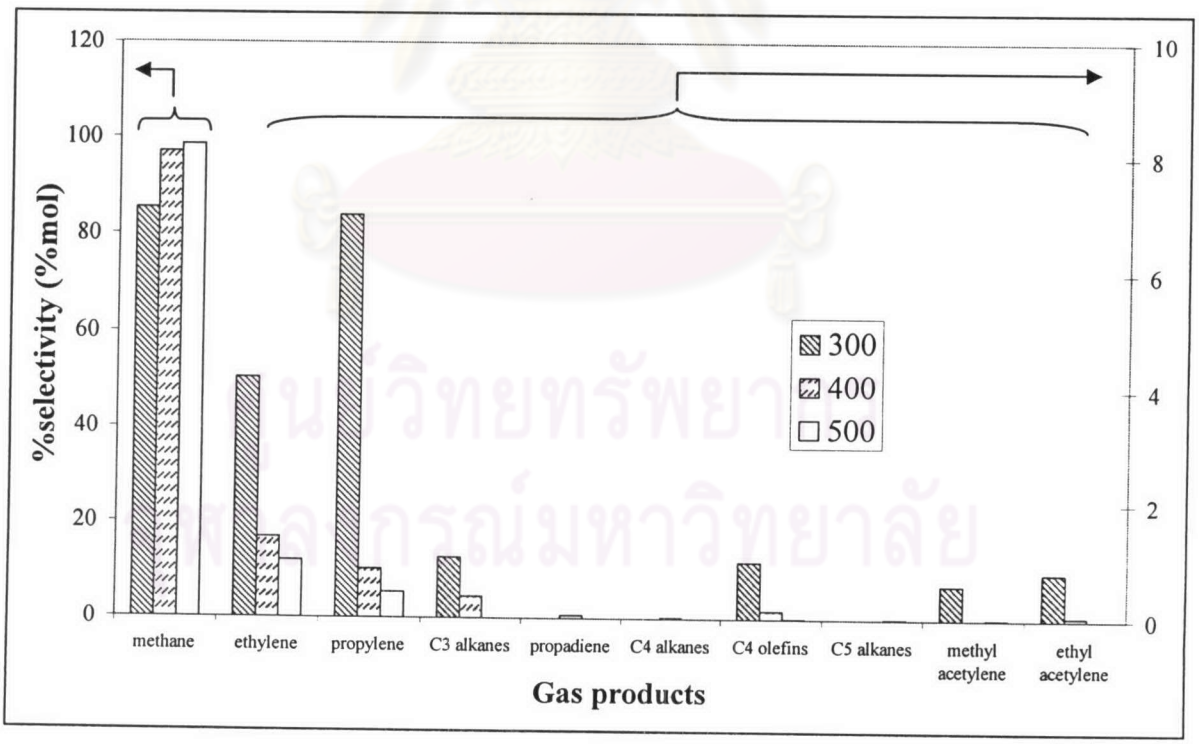

Figure 4.21 The gas products distribution obtained from the methanol conversion over Fe-SBA-15 (Si/Fe in gel = 90 and Fe^{3+} as iron source) at various temperatures and the same condition as shown in Table 4.4.

4.2.2 Effects of iron source on the methanol conversion

To prove the effect of iron sources, two Fe-SBA-15 materials synthesized with different iron sources are tested in methanol conversion. The Fe-SBA-15 materials synthesized at following conditions: Si/Fe molar ratio in gel of 180, pH of gel of 2.5, with Fe^{3+} and Fe^{2+} as iron sources are used as catalysts because they were synthesized under the same condition and the Si/Fe molar ratios in catalyst are almost the same (Si/Fe = 222-223). The reaction was performed at the reaction temperature of 300 °C. The results are shown in Table 4.5 and the gas product distribution is shown in Figure 4.22.

Similar catalytic results for both Fe-SBA-15 catalysts prepared by using Fe^{2+} and Fe^{3+} as iron source indicate that the difference of iron source does not affect the methanol conversion and product distribution. The reason is that Fe^{2+} is completely converted to Fe^{3+} during calcination in oxygen to remove organic template, resulting in pale yellow catalysts for both type of catalysts. Moreover, during crystallization at 100 °C it is found that Fe^{2+} is oxidized to Fe^{3+}, so the use of different iron sources does not influence the catalytic activity of Fe-SBA-15 in methanol conversion.

Table 4.5 Percentage conversion, product distribution, and coke content obtained from the methanol conversion over Fe-SBA-15 (Si/Fe = 222-223) synthesized from Fe^{2+} and Fe^{3+} as iron sources (Conditions: 0.25 g catalyst, GHSV = 2000 h^{-1}, $T_{reaction}$ = 300 °C, T_{MeOH} = 35°C, and TOS = 30 min)

	Iron source	
	Fe^{3+}	Fe^{2+}
%Conversion of methanol	23.87	23.76
% Product distribution		
selectivity to:	54.67	54.61
- Gas product yield (%wt.)	7.00	7.05
- Liquid product yield (%wt.)	38.33	38.34
- Coke yield (%wt)		
% Coke based on catalyst	4.61	4.63

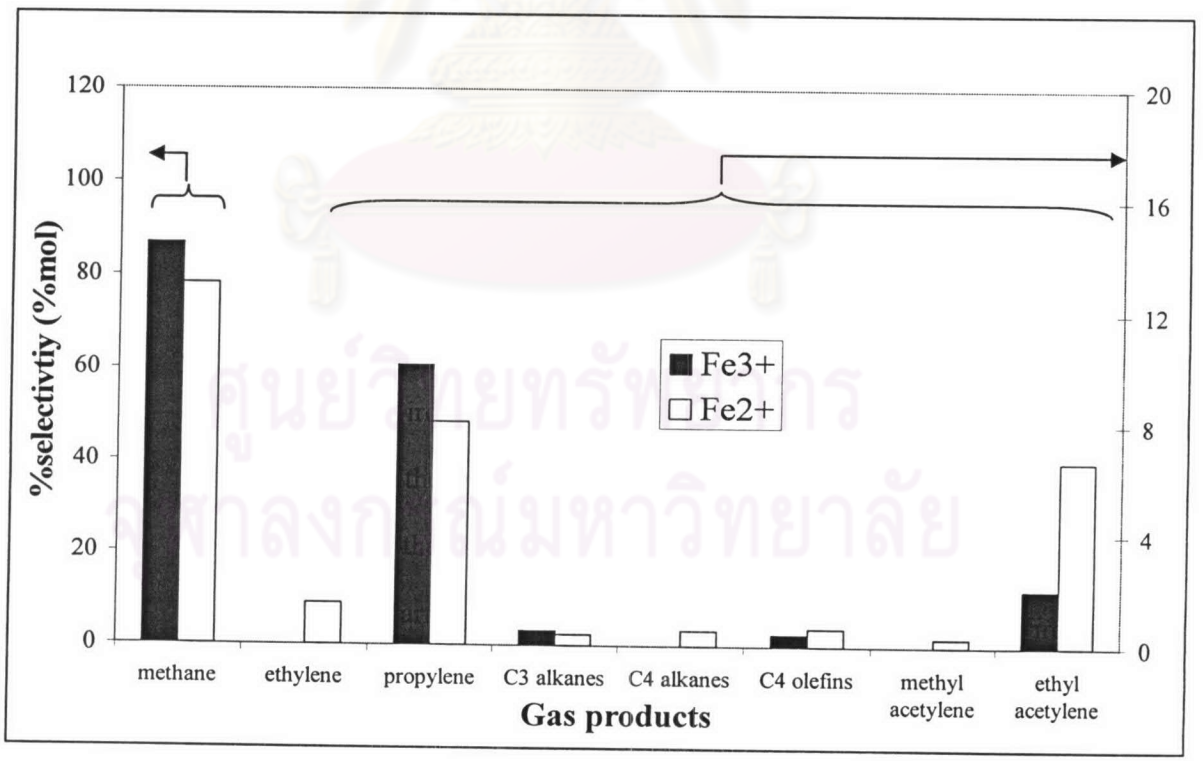

Figure 4.22 The gas products distribution obtained from the methanol conversion over Fe-SBA-15 synthesized from Fe^{2+} and Fe^{3+} as iron source and the same condition as shown in Table 4.5.